Quantitative Analyses of Cell Aggregation Behavior Using Cell Trajectory Data(Dissertation_全文)

AUTHOR(S):

Otaka, Akihisa

Quantitative Analyses of Cell Aggregation Behavior Using Cell Trajectory Data

Akihisa OTAKA

Graduate school of engineering

Kyoto University

TABLE OF CONTENTS

Chapter 1.
General introduction

1.1. TISSUE ENGINEERING AND ITS CHARANGES

The loss or failure of a tissue is one of the most frequent, devastating, and costly problems in human health care. Tissue engineering applies the principles of biology and engineering to the development of functional substitutes for dysfunctional tissue (1). It was reported that an almost three-fold growth in commercial sales over the past 4 years. In addition, the number of companies selling products or offering services has increased over two-fold to 10^6, and they are generating a remarkable $3.5 billion in sales (2).

Cell-based therapy is one of major approaches, in which substitute function is recreated using living cells. The premise of live cells as a therapeutic agent requires the harnessing of a cell's elegant biochemical mechanical machinery to perform functions that cannot be mimicked by exogenous drug products or surgical intervention, or to use the cell's replicative ability for cell production and tissue replacement (3). Langer et al. reported that three general strategies have been adopted for the creation of new tissue: (a) isolated cells or cell substitutes, (b) tissue-inducing substances, and (c) cells placed on or within matrices (1). In the third strategy, cell scaffolds have been essential components and they provide not only provide 3D space for cell attachment but also induce subsequent tissue formation. Scaffold influences cell differentiation, proliferation, survival, and migration through biochemical and mechanical interactions (4). Successful understanding of this interaction will facilitate the ability to guide cell behavior and proper tissue formation.

1.2. CELL AGGREGATION BEHAVIOR

Cell aggregation/condensation process is a pivotal stage in the tissues development (5–7). Cell aggregates are also important tools in the study of tissue development, permitting correlation of cell-cell interactions with cell differentiation, viability and migration, as well as subsequent tissue formation. The aggregate morphology permits re-establishment of the cell-cell contacts normally present in tissues; therefore, cell function and survival are often enhanced in aggregate culture. Because of this, cell aggregates may also be useful in tissue engineering, enhancing the function of cell-based hybrid artificial organs or reconstituted

tissue transplants (8).

Cell aggregate formation have been observed on various materials (9–11). Kawakami et al. evaluated chondrocyte distribution in fibroin substrates, and showed that chondrocytes formed cell aggregates in the sponge within 24 h after seeding and that cartilage tissue was formed later around those aggregates (9). It is generally said that extracellular matrix molecules, cell surface receptors and cell adhesion molecules initiate condensation formation and set condensation boundaries (5, 12–14). Therefore, understanding of cell aggregate formation process are important tools in the study of tissue development, permitting correlation of cell-cell interactions with cell differentiation, viability and migration, as well as subsequent tissue formation within scaffold. However, when it came to figuring out cell aggregation behavior, there are few analytical methods to evaluate cell aggregation observed in each study.

Cell trajectory analysis is a powerful tool and has been used in order to investigate the effect of cell's microenvironment (e.g., its matrix or cytokine) on cell motility. On the other hand, these researches were performed under low-cell-density conditions in order to minimize any cell-cell interactions over the course of the experiment. Therefore, cell aggregation mechanisms remain yet to be clarified because of lack of quantitative method of cell aggregate formation.

1.3. SCOPE OF THE STUDY

This thesis proposes several quantitative analyses for cell aggregation behavior, and cell aggregate formation on fibroin scaffold material was evaluated. Three main approaches were performed: (a) quantification using Voronoi diagram analysis, (b) quantification focusing on cell-cell distance, and (c) quantification focusing on the direction of cell migration. In the first part (chapter 2), the concept of "cellular sociology" was introduced into tissue engineering and bio-environment design, and a cell distribution assay, which has been used in the field of cellular sociology, was examined with respect to its validity as a method for evaluating chondrocyte aggregation. Voronoi diagram analysis proved to be successful in identifying global cell aggregation behavior. However, this technique was insufficient for evaluating the specific behavior of individual cells during aggregation, because the technique focuses on the overall spatial distribution of cells rather than individual cell behavior during aggregate formation. Therefore, in the second part (chapter 3 and 4), Moving-Points Grouping Method (MPGM) and co-migration analysis were introduced, and cell-cell distance and its dynamic changes was quantitatively investigated in order to characterize cell

aggregation process. The third part, in chapter 5, introduces a new method to detect cell attractive behavior based on a Density-Based Cellular Automaton Model (15). The relationship between cell migration velocity and cell density gradient was evaluated in order to evaluate cell aggregation behavior caused by attractive motility.

1.4. REFERENCES

1. Langer, R., and J. Vacanti. 1993. Tissue engineering. Science (80-.). 260: 920–926.

2. Jaklenec, A., A. Stamp, E. Deweerd, A. Sherwin, and R. Langer. 2012. Progress in the tissue engineering and stem cell industry “are we there yet?”Tissue Eng. Part B. Rev. 18: 155–166.

3. Palsson, B.O., and S.N. Bhatia. 2003. Tissue Engineering. Prentice Hall.

4. Owen, S.C., and M.S. Shoichet. 2010. Design of three-dimensional biomimetic scaffolds. J. Biomed. Mater. Res. A. 94: 1321–1331.

5. Hall, B.K., and T. Miyake. 2000. All for one and one for all: condensations and the initiation of skeletal development. Bioessays. 22: 138–47.

6. Maleski, M., and C.B. KNUDSON. 1996. Hyaluronan-mediated aggregation of limb bud mesenchyme and mesenchymal condensation during chondrogenesis. Exp. Cell Res. 66: 55–66.

7. Knothe Tate, M.L., T.D. Falls, S.H. McBride, R. Atit, and U.R. Knothe. 2008. Mechanical modulation of osteochondroprogenitor cell fate. Int. J. Biochem. Cell Biol. 40: 2720–38.

8. 2013. Principles of Tissue Engineering, 4th Edition. Academic Press.

9. Kawakami, M., N. Tomita, Y. Shimada, K. Yamamoto, Y. Tamada, et al. 2011. Chondrocyte distribution and cartilage regeneration in silk fibroin sponge. Biomed. Mater. Eng. 21: 53–61.

10. Brun, P., G. Abatangelo, M. Radice, V. Zacchi, D. Guidolin, et al. 1999. Chondrocyte aggregation and reorganization into three-dimensional scaffolds. J. Biomed. Mater. Res. 46: 337–46.

11. Kachi, N.D., A. Otaka, S. Sim, Y. Kuwana, Y. Tamada, et al. 2010. Observation of chondrocyte aggregate formation and internal structure on micropatterned fibroin-coated surface. Biomed. Mater. Eng. 20: 55–63.

12. Lauffenburger, D. a, and L.G. Griffith. 2001. Who's got pull around here? Cell organization in development and tissue engineering. Proc. Natl. Acad. Sci. U. S. A. 98: 4282–4.

13. Ryan, P.L., R.A. Foty, J. Kohn, and M.S. Steinberg. 2001. Tissue spreading on implantable substrates is a competitive outcome of cell-cell vs. cell-substratum adhesivity. Proc. Natl. Acad. Sci. U. S. A. 98: 4323–4327.

14. Kim, M.-H., M. Kino-oka, Y. Morinaga, Y. Sawada, M. Kawase, et al. 2009. Morphological regulation and aggregate formation of rabbit chondrocytes on dendrimer-immobilized surfaces with D-glucose display. J. Biosci. Bioeng. 107: 196–205.

15. Bonnet, N., M. Matos, M. Polette, J.-M. Zahm, B. Nawrocki-Raby, et al. 2004. A density-based cellular automaton model for studying the clustering of noninvasive cells. IEEE Trans. Biomed. Eng. 51: 1274–1276.

Chapter 2.
Observation and quantification of chondrocyte aggregation behavior on fibroin surfaces using Voronoi partition

2.1. INTRODUCTION

Live cell observation has become a powerful analytical tool in many cell biology laboratories because of advancements in microscopy techniques and cell imaging technologies (1). On the other hand, evaluation methods for quantifying multicellular morphodynamics are still not yet fully developed. However, in order to successfully engineer artificial tissue constructs, some quantification tools for analyzing multicellular formation are required (2).

For accurately evaluating the spatio-temporal formation of cell populations there are two major requirements. First, automated visual tracking of the cells is necessary for quantitative and systematic analysis. Second, techniques that accurately characterize patterns of cell behavior, such as migration, proliferation, and apoptosis, are required. While visual tracking techniques have been studied extensively, less attention has been given to cell behavior characterization techniques.

In previous work, Kawakami et al. demonstrated that initial chondrocyte aggregation led to enhanced cartilage tissue formation in fibroin sponges (3). Additionally, cell aggregation is considered to be a key event in a wide range of fields, from tissue engineering to embryology and involves many types of cells, such as hepatocytes and chondrocytes (3–5), as along with tumor and mesenchymal stem cells as well. This indicates that cell aggregation is one of the key events in cell-to-cell interaction, making it a vital part of tissue formation. However, in multicellular biophysics, evaluation of the cell aggregation process has been neither quantitative nor objective, but rather qualitative and highly researcher dependent. This lack of reliable and repeatable quantitative cell aggregation assays has made it difficult to investigate multicellular biophysics in the aggregate formation process.

The purpose of this chapter was to introduce the concept of "cellular sociology" into tissue engineering and bio-environment design. This concept focuses on the “social” behavior of cell populations, which varies in response to the cells’ surroundings and the physiological and phenotypical state of the cells themselves. Moreover, by understanding the relationship between cell population and extracellular environment, it is possible to gain insights into a

wide range of cell biophysics (e.g., cell-cell and cell-substrate/material interactions). In the field of cellular sociology, cell arrangement analysis using a Voronoi diagram is one of the most successful methods for the evaluation of different cell populations. Voronoi analysis has been used previously to evaluate the spatio distribution of retinal (6), cortical (7) and tumor cells (8–11). Raby et al. evaluated the process of tumor cell cohesion using graphical quantification, including Voronoi diagram analysis, and concluded that this method represented a new way to predict the aggressiveness of various tumor cells (9). In a similar fashion, Voronoi diagram analysis may provide new insights into the multicellular biophysics involved in tissue regeneration and allow for improved computational modeling of cell behavior in scaffolds.

In this chapter, two types of experiments were performed. First, Marcelpoil's distribution assay (12), which has been used in the study of tumor cell distribution (9, 11), was examined with respect to its validity as a method for evaluating chondrocyte aggregation on different substrates. Specifically, in order to confirm the relationship between cell aggregation and various analysis metrics, unambiguous examples of different aggregation patterns were simulated and analyzed in a set of in silico experiments. After confirming these relationships, a number of in vitro experiments were then performed to examine the spatio-temporal distributions of chondrocytes on three different substrates: (a) collagen; (b) fibroin; and (c) RGD-transgenic fibroin, which was created by genetically interfusing arginine-glycine-aspartic acid-serine (RGDS) peptides into silk fibroin molecules (13). It was reported previously that chondrocyte aggregation is enhanced in fibroin sponges (3), but chondrocyte aggregation behavior on fibroin has yet to be evaluated quantitatively. Thus, the objective of this study was to quantitatively assess whether fibroin enhances cell aggregation behavior using in silico validated Voronoi diagram analysis methods.

2.2. MATERIALS AND METHODS

2.2.1. Cell population quantification

The spatial distribution of cells was characterized and quantified using a cellular sociology algorithm based on geometrical models, as described by Marcelpoil et al. (12) (i.e. Voronoi's partition). These methods, applied to the set of points that relate to the position of the cells (Fig. 2.1), provide information about the spatial distribution and neighborhood relationships of the cells. From the Voronoi diagram, three quantitative parameters can be deduced: (a) average and standard deviation of the areas (RFav); (b) roundness factor

homogeneity (RFH); and (c) area disorder (AD). Each index was calculated using the equations derived by Marcelpoil et al. (12). As is customary, border zones of the Voronoi diagram were excluded from the analysis, as no information can be taken relating to the final position of cells in these zones.

2.2.2. *In silico* experiment: Simulation of aggregate cell populations

2.2.2.1. Model formulation

Cell aggregations can vary in their size, cell density and gathering potential. A computer simulation model was conducted to examine whether cell population affects the RFav, RFH, and AD indexes during aggregation. Three cell population models (type A, type B and type C; described in 2.2.2.2) that were observed regularly in our time-lapse observation were simulated. Afterward, the cell distribution points were evaluated using a Voronoi diagram. Every trial was executed and evaluated six times.

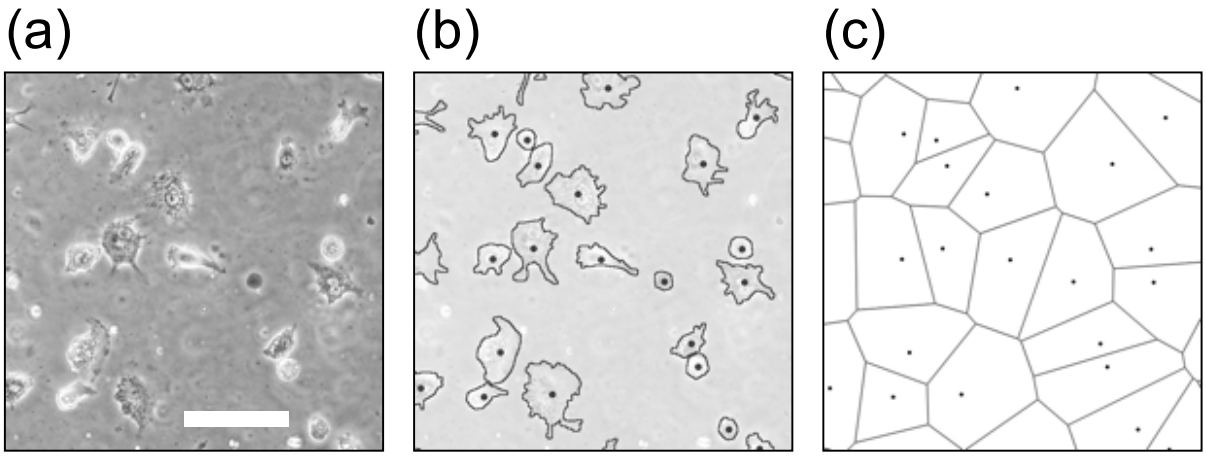

Fig. 2.1 Representation of the data acquisition process. (a): Example of typical cartilage observation on a PDMS surface with a phase-contrast microscope. (b): Outlines and center points of cells extracted from snapshot images. (c): The derived Voronoi polygon using the point set of cell centers created by the Open Computer Vision Library (http://opencv.willowgarage.com/wiki/). Scale bar = 20 μm.

2.2.2.2. Model of cell arrangement

Three types of cell distribution were created using 100 separate points set on a 2D plane using the procedures described below. Cells were not placed at the exact nodal points of the square lattice, but rather randomly scattered around each node using a Gaussian distribution with a standard deviation of 10 pixels (Fig. 2.2).

Type A: This model was used to analyze the effect of cell density. Using a 10X10 array of points located at the nodes of a perfect square lattice, groups with high, medium, and low cell density were simulated by changing the mesh size of the square lattice to 30 (high density; H), 60 (middle density; M), and 90 pixels (low density; L), respectively. A control group (C) in which the population was distributed randomly (Fig. 2.3 model A) was also created.

Type B: This model was used to evaluate the rate at which cells participated in aggregation. Using an array of N points located at the nodes of a square lattice and 100-N points distributed randomly, groups with 0%, 25%, 50%, 75% and 100% aggregation participation ratios were simulated by changing the *N* value to 0, 25, 50, 75 and 100, respectively (Fig. 2.3 model B).

Type C: This model was used to analyze the effect of aggregate size. Using point forming groups, three types of cell populations were created in which cells formed: 1 large aggregate (AGG:1); 2 smaller aggregates (AGG:2); and 4 aggregates (AGG:4) that were smaller still. Each nodule had the same size, and contained 100, 50 and 25 points, respectively (Fig. 2.3 model C).

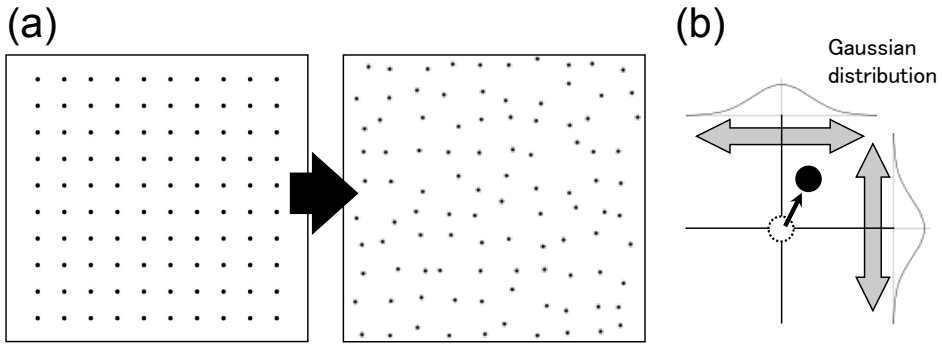

Fig. 2.2 Schematic model of an aggregating cell population. (a): Randomization of the point set ordered at the nodes of a square lattice. (b): Spatial perturbation of a point in XY coordinates according to the Gaussian distribution with a standard deviation of 10 pixels.

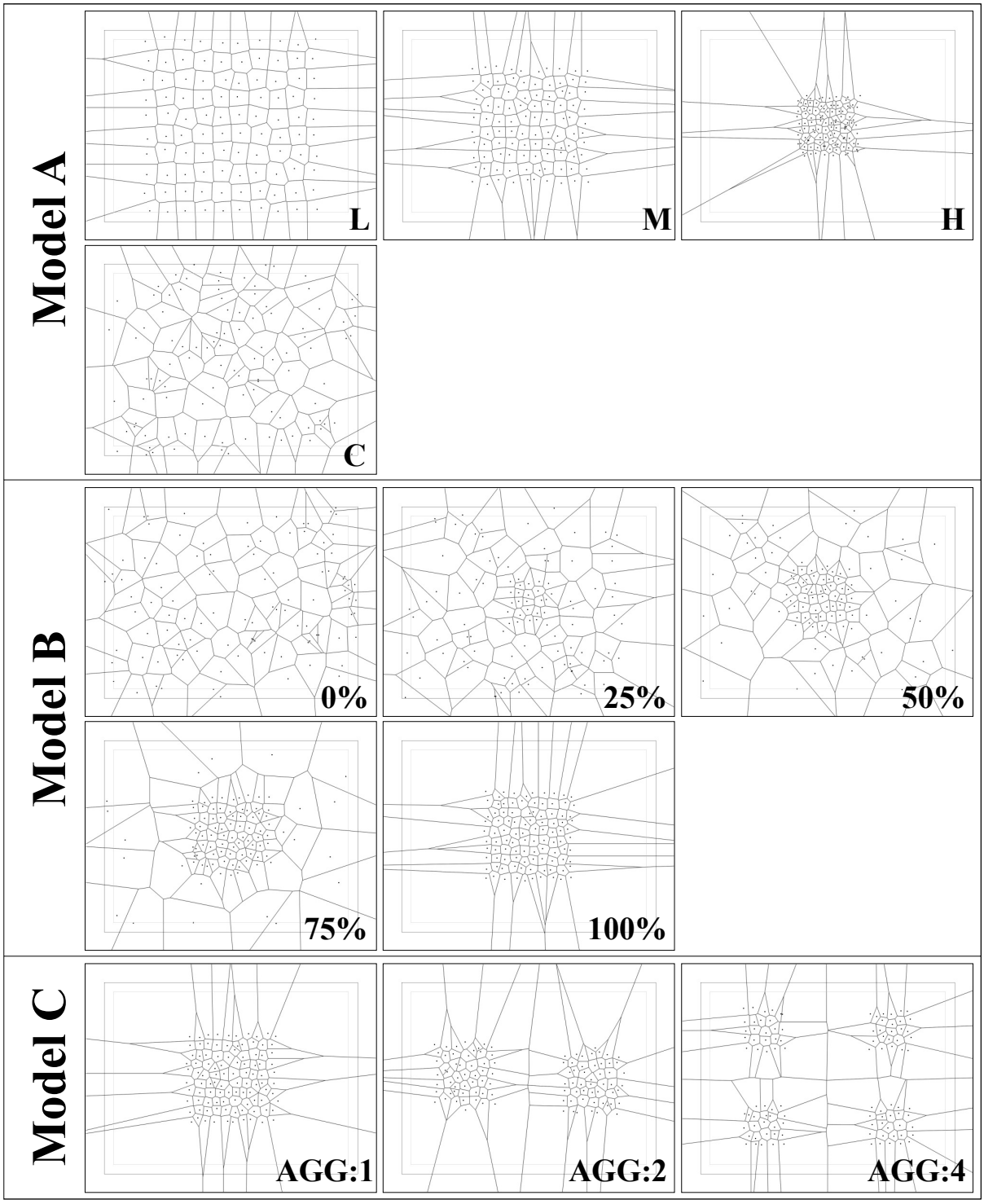

Fig. 2.3 Representative image of aggregation models. Each model was varied in the degree of cell density (type A), cell aggregation participation ratio (type B) and the number of cells within each aggregate (type C).

2.2.3. *In vitro* experiment: Cell seeding experiment in 2D culture

2.2.3.1. Chondrocyte preparation

Articular cartilage tissue was aseptically removed from the proximal humerus, distal femur, and proximal tibia of 4-week-old Japanese White rabbits (Oriental Bio Service Co., Ltd., Japan). After any adherent connective tissue had been removed, the excised cartilage tissue was diced into 1 mm3 segments and chondrocytes were isolated by digesting small segments of cartilage with 0.25% trypsin-EDTA (Nacalai Tesque, Inc., Japan) for 30 minutes in a temperature-controlled bath at 37°C. After being rinsed twice with Dulbecco's Phosphate Buffered Saline (PBS; Nacalai Tesque, Inc., Japan) and centrifuged at 1500 rpm for 5 minutes, the cartilage was enzymatically digested with 0.25% type II collagenase (CLS-2, Worthington Biochemical Co., USA) for 6 hours at 37°C. After staining through a cell strainer (BD Falcon, Inc., USA) and washing twice with PBS, a single-cell suspension was obtained. Cartilage harvests from living animals were approved and accepted by the animal care committee of the Institute for Frontier Medical Sciences at Kyoto University.

Cells were passaged once in T-flasks (IWAKI Glass Co., Ltd., Japan) with Dulbecco's modified Eagle's medium (DMEM; Nacalai Tesque, Inc., Japan) containing 10% fetal bovine serum (FBS; Nacalai Tesque, Inc. Japan) and 1% antibiotic mixture (10,000 units/ml penicillin, 10,000 mg/ml streptomycin, and 25 mg/ml amphotericin B; Nacalai Tesque, Inc., Japan) prior to experimentation. Cells were cultured at 37°C in a humidified atmosphere of 95% air and 5% CO2 for 5 days, and the medium changed every 2 days.

2.2.3.2. Substrate preparation

A polydimethylsiloxane (PDMS) liquid solution was prepared by using a SYLGARD 184 SILICONE ELASTOMER KIT (Dow Corning Toray Co., Ltd., Japan) and curing for 48 hours at room temperature in a culture dish (diameter, 150 mm; Asahi Glass Co., Ltd., Japan). Afterward, the PDMS sheet was cut into disks that were 2 mm in thickness and 35 mm in diameter. Disks were sterilized by autoclave before experimentation.

Collagen (CON), wild-type fibroin (FIB), and L-RGDSx2 fibroin (LRF) were used as substrate coatings and prepared using the procedures listed below. Three substrate-coated disks were prepared for each substrate (CON, FIB and LRF) and set in a culture dish (diameter, 35 mm; Asahi Glass Co., Ltd., Japan). Each substrate disk was washed twice with PBS before use.

Collagen substrate: As a control, type I collagen coated PDMS disks were used, with PDMS chosen due to its hydrophobic nature. The PDMS disks were soaked in 10%

Cellmatrix Type I-C (Nitta gelatin Inc., Japan) diluted in HCl (pH3.0, 1mM) for 30 minutes at room temperature. Afterwards the plates were washed with culture medium (DMEM) three times and with PBS twice thereafter.

Fibroin substrate: A fibroin aqueous solution was prepared as described previously (5, 20). Briefly, degummed silk fibroin fibers from *Bombyx mori* cocoons were dissolved in a 9 M lithium bromide aqueous solution at room temperature, with the solution subsequently dialyzed against pure water. The concentration of fibroin in the water solution was determined by colorimetric method and was prepared to be 1 % (wt/vol). Before coating the fibroin substrate, PDMS disks were treated with O_2 plasma in order to make the surface hydrophilic. The PDMS disks were then soaked in the fibroin aqueous solution for 1 hour at room temperature, and dried at 50°C. The coated disks were immersed in an 80% methanol solution for 1 hour, and dried again at 50°C.

L-RGDSx2 fibroin substrate: The L-RGDSx2 fibroin is a protein in which (RGDS)x2 sequences have been fused with fibroin L-chains at the amino-terminus. An L-RGDSx2 fibroin aqueous solution was prepared using the same technique as that used for the preparation of the wild-type fibroin aqueous solution. PDMS disks coated with L-RGDSx2 fibroin were also manufactured in the same process as that used for of the wild-type fibroin samples.

2.2.3.3. Time-lapse microscopy

Passaged chondrocytes were removed from T-flasks by adding 0.25% trypsin-EDTA and washing twice with PBS. Shortly after detachment, cells were suspended in Leibovitz's L-15 medium (Invitrogen Corp., USA) containing 10 vol% Fetal Bovine Serum, and 1 vol% antibiotic mixture and seeded on substrate dishes at a concentration of $1.5x10^4$ cells/cm^2. Following that, the dish was placed on an inversion microscope (IX-71; Olympus Corp., Japan) and enclosed in a small transparent culture chamber (MI-IBC-IF; Olympus Corp., Japan) with in a humidified atmosphere at 37°C. A 10X magnification objective lens (CPlan N 10x/0.25 PhC; Olympus Corp., Japan) was used in our experiment. During a 24-hour culture, time-lapse phase contrast images were captured every 10 minutes by a CCD camera (DP70; Olympus Corp., Japan).

2.2.3.4. Chondrocyte distribution quantitation

To acquire positional datum related to the chondrocytes' distribution, the images, captured at 10 minutes, and 3, 6, 9, 12 and 24 hours after seeding, were analyzed according to the following procedure. Each cell was outlined and painted over manually using Photoshop (Adobe Systems Inc., Japan) and cell binary images were generated. Afterward, the cell positions were sorted out using the Particles Analysis command in ImageJ (National

Institutes of Health, USA) (Fig. 2.1). Using this population data, Voronoi diagrams were produced and three indexes (AD, RFav, RFH) were calculated. The number of cells was also recorded, and the rate of cell growth was calculated by dividing the number of cells in each time step by the initial number of cells. Time-dependent changes in AD were fitted to a nonlinear regression model.

2.2.4. Statistical analysis and data presentation

Experimental values in each figure are presented as mean ± SD. One-way analysis of variance and a Tukey test for post hoc comparison were done to analyze the significance of time dependent changes in RFH, RFav, AD and the rate of cell growth *in vitro* experiments. A Student's t-test was done to analyze the significance between the groups in the *in vitro* experiment. All statistical tests were determined using a criterion of $p < 0.05$. An asymptotic exponential curve was used for regression analysis of the temporal AD changes on each substrate.

2.3. RESULTS

2.3.1. The outcomes from *in silico* experiments

The RFav vs. RFH vs. AD Diagram shown in Fig. 2.4 describes the results for RVav, RFH and AD in the in silico experiments. These results were calculated from cell simulations using type A (Fig. 2.4 a), type B (Fig. 2.4 b) and type C (Fig. 2.4 c) cell populations. In these conditions, RFav, RFH and AD ranged from 0.65 to 0.80, from 0.74 to 0.90 and from 0.31 to 0.72, respectively.

The statistical significance analysis indicates that RFav is insensitive to the rate at which cells participate in aggregation (Fig. 2.4 b), and that RFH is insensitive to the number of cells involved in aggregation (Fig. 2.4 c). On the other hand, AD results reveal a significant difference between multiple groups for all simulation types. Thus, AD appears to be more sensitive than RFav and RFH in evaluating aggregating cell populations, especially with respect to aggregate cell density and the ratio of cells involved in aggregation.

2.3.2. The outcomes from *in vitro* experiments

In Fig. 2.5, chondrocytes on each substrate are shown after 12 and 24 hours of culture time. On the collagen substrate, chondrocytes elongated and few cells were found to be in

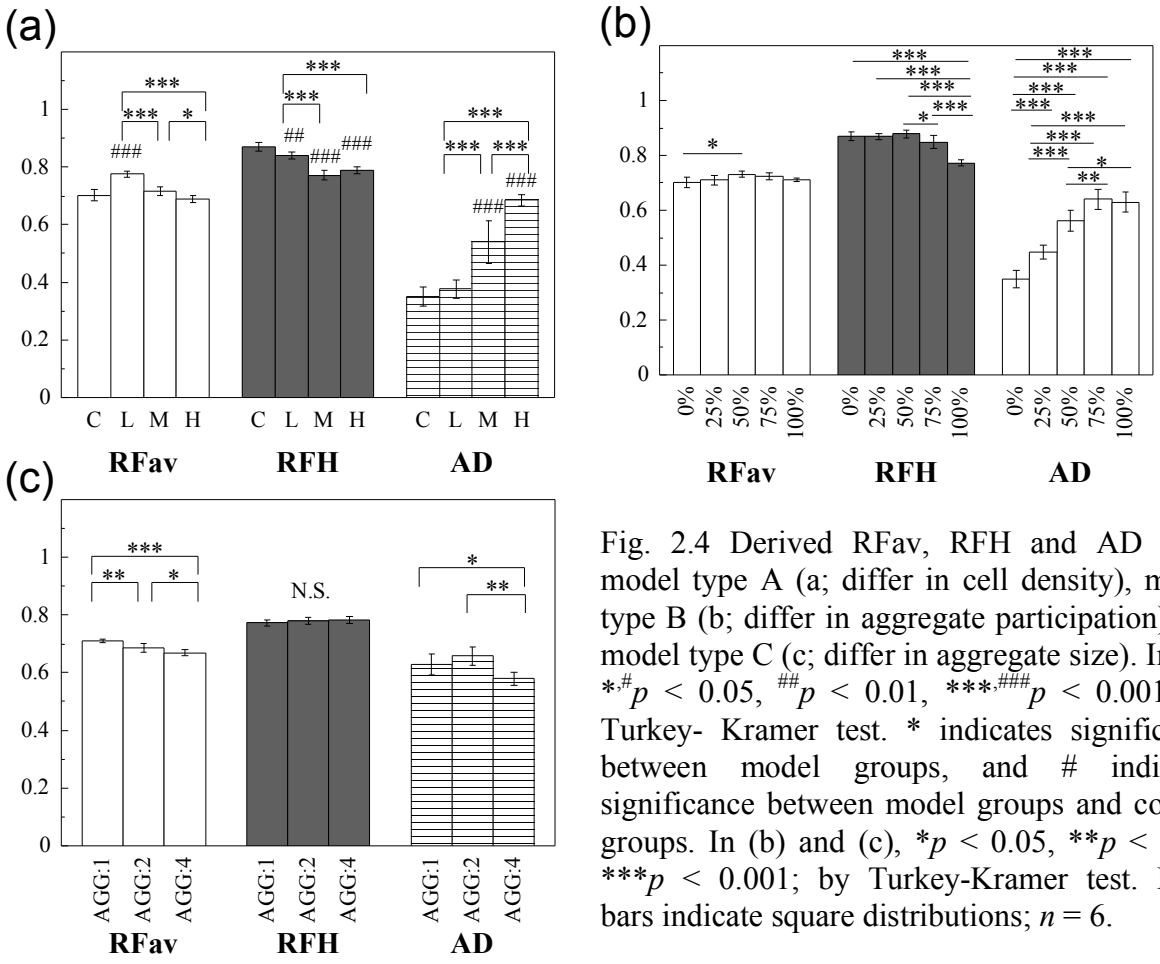

Fig. 2.4 Derived RFav, RFH and AD from model type A (a; differ in cell density), model type B (b; differ in aggregate participation) and model type C (c; differ in aggregate size). In (a), $*^{,\#}p < 0.05$, $^{\#\#}p < 0.01$, $***^{,\#\#\#}p < 0.001$; by Turkey- Kramer test. * indicates significance between model groups, and # indicates significance between model groups and control groups. In (b) and (c), $*p < 0.05$, $**p < 0.01$, $***p < 0.001$; by Turkey-Kramer test. Error bars indicate square distributions; $n = 6$.

contact with each other (CON). On both fibroin substrates (FIB and LRF), most chondrocytes maintained a rounded shape and participated in cell aggregation. Chondrocytes on these substrates were active in migration during the early stages of cell culture, but cell speed appeared to decrease with cell aggregation. Compared with the LRF substrate, the aggregation size was larger and fewer cells remained solitary on the FIB substrate.

Chondrocytes on the FIB and LRF substrates didn't increase significantly in the 24-hour culture period, as shown in Fig. 2.6. Only on the collagen substrate was significant cell growth observed ($p < 0.01$, one-way ANOVA). Furthermore, significant differences in the temporal cell growth on the collagen substrate were found only between 10 minutes – 24 hours ($p < 0.01$), 3 hours – 24 hours ($p < 0.01$) and 12 hours – 24 hours ($p < 0.05$, Turkey test) of culture time. Thus, there were no significant changes in cell proliferation during the first 12 hours after seeding on each surface.

The time-dependent changes in RFav, RFH and AD for chondrocytes grown on each substrate are shown in Fig. 2.7. The initial value for each index was almost the same for each substrate, but the RFav and AD values for the FIB substrate and all three indices for the LRF substrate changed significantly over the 24-hour culture period ($p < 0.05$, one-way anova).

The absence of change in the indexes recorded for the CON substrates was probably caused by the cells lack of aggregation. Asymptotic exponential curves were fitted to the mean values of the AD index in a time-dependent manner for every substrate (Fig. 2.8.) The relaxation time was 1.56 for the FIB substrate and 4.39 for the LRF substrate, and the AD values for the FIB and LRF substrates were fixed at 0.54 and 0.49, respectively during the 24-hour culture period.

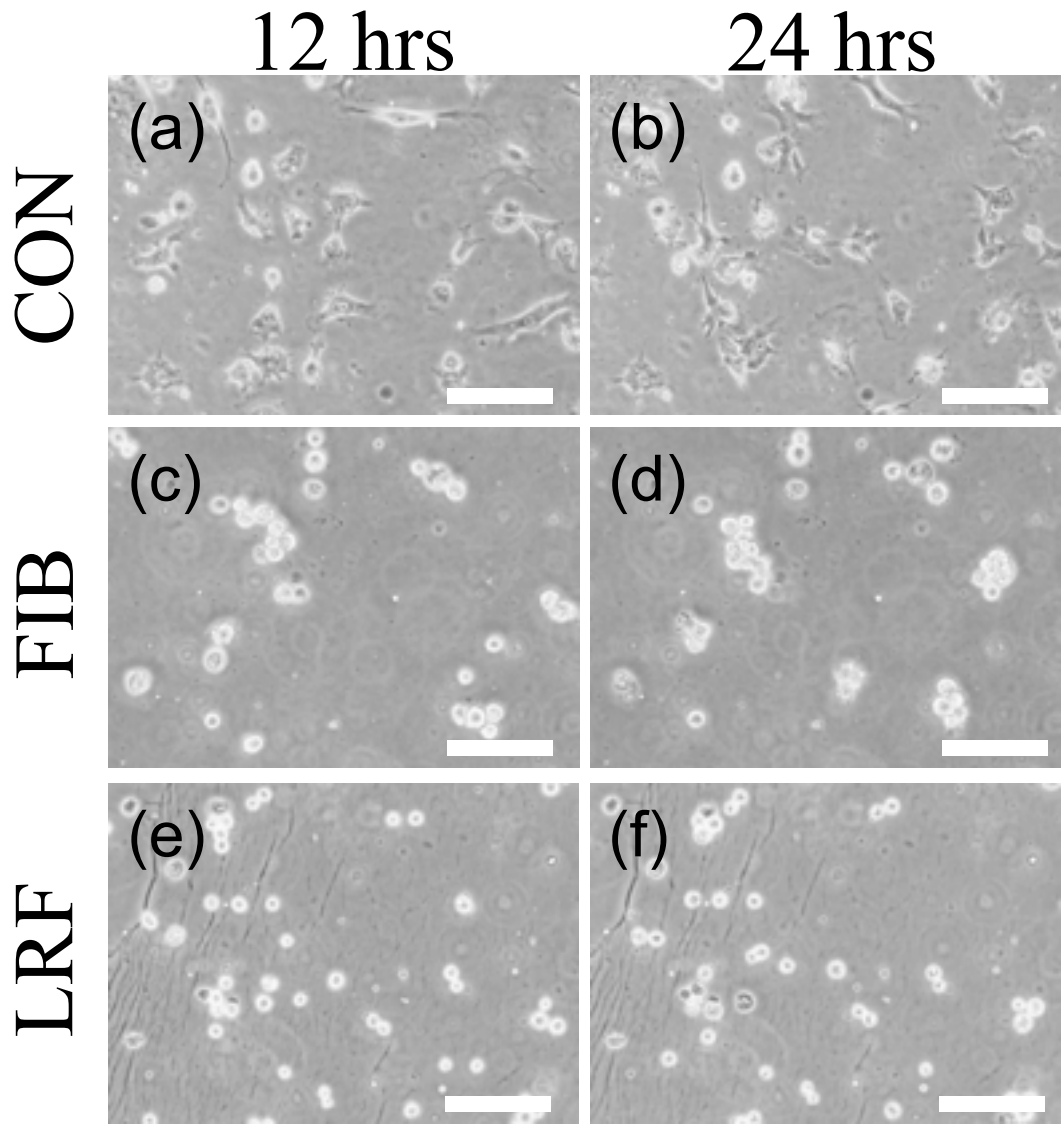

Fig. 2.5 Phase contrast images of chondrocytes cultured on collagen (a and b), on wild-type fibroin (c and d) and on RGD fibroin surfaces (e and f), which were taken 12 hours (a, c and e) and 24 hours (b, d and f) after seeding. Scale bar = 20 μm.

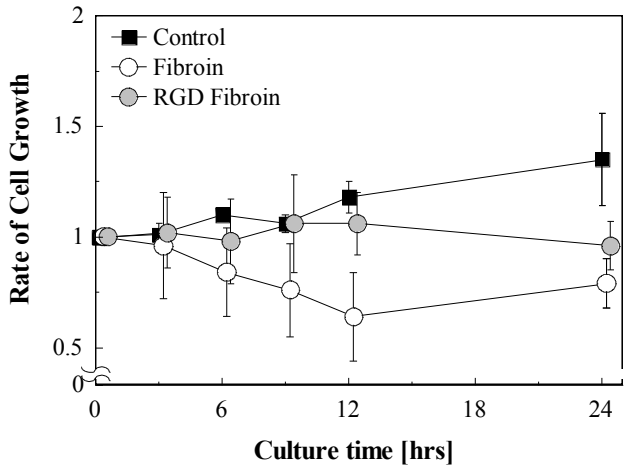

Fig. 2.6 Temporal changes in chondrocyte growth rate on each substrate. The significant change in the number of observed chondrocytes was seen only on the collagen surface by one-way ANOVA. Error bars indicate square distributions; $n = 3$.

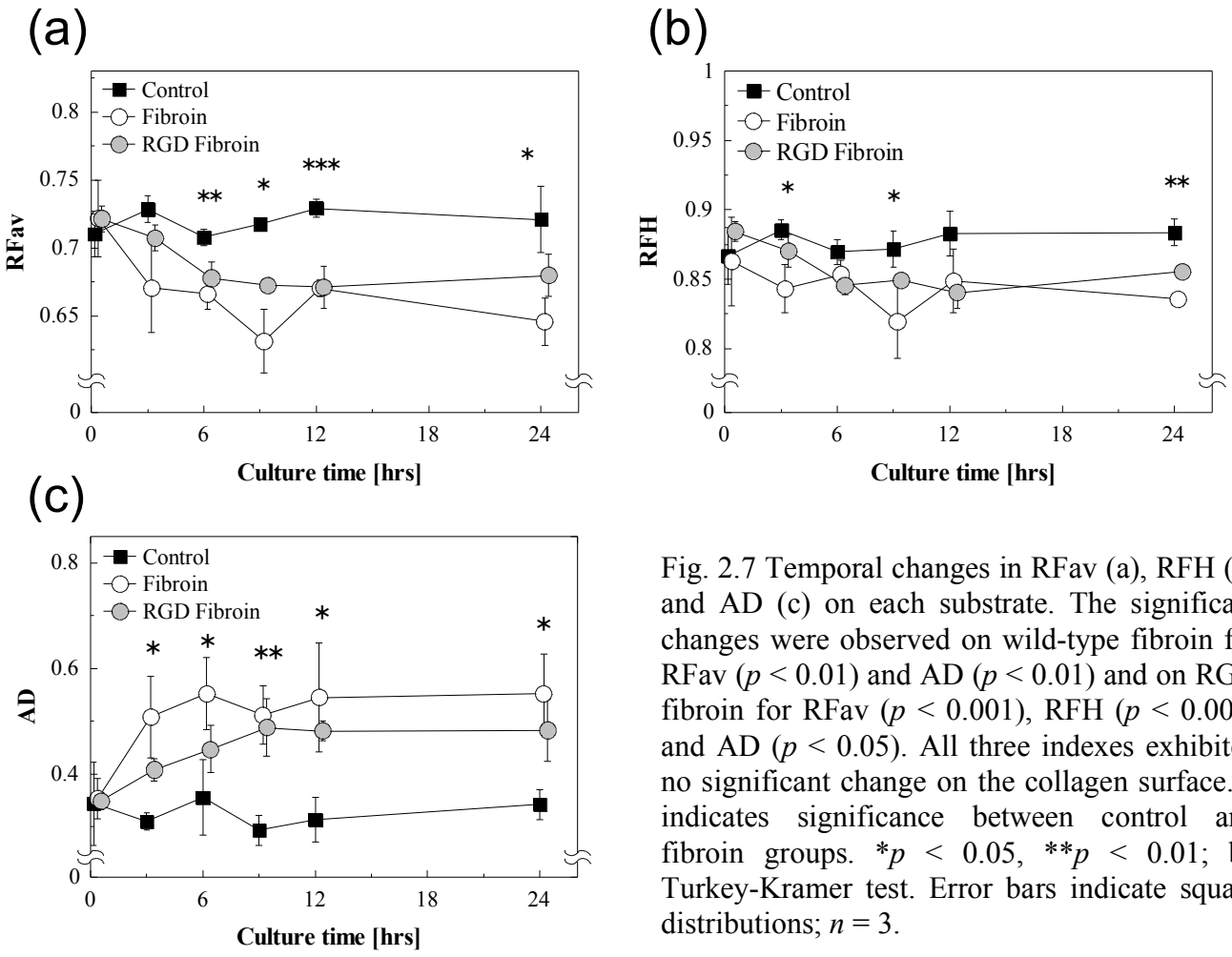

Fig. 2.7 Temporal changes in RFav (a), RFH (b) and AD (c) on each substrate. The significant changes were observed on wild-type fibroin for RFav ($p < 0.01$) and AD ($p < 0.01$) and on RGD fibroin for RFav ($p < 0.001$), RFH ($p < 0.001$) and AD ($p < 0.05$). All three indexes exhibited no significant change on the collagen surface. * indicates significance between control and fibroin groups. *$p < 0.05$, **$p < 0.01$; by Turkey-Kramer test. Error bars indicate square distributions; $n = 3$.

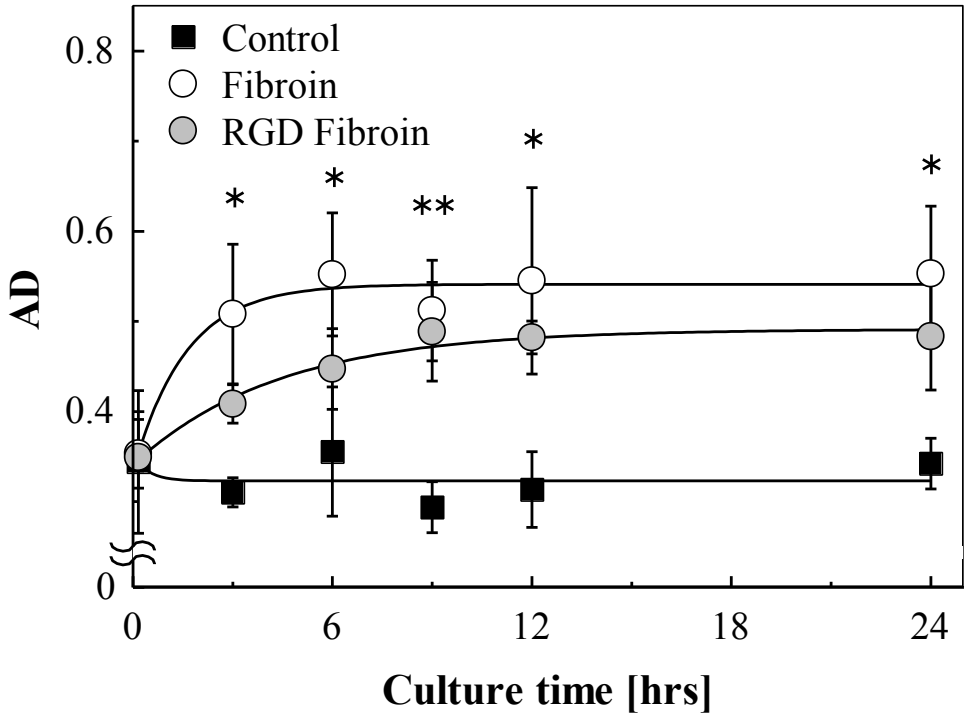

Fig. 2.8 Regression analysis of temporal AD changes for each substrate, resulting in a fit with R_2 of 0.13 (collagen), 0.96 (wild-type fibroin) and 0.99 (RGD fibroin). Each AD value converged to 0.32, 0.54 and 0.49, with a relaxation time of 0.44, 1.56 and 4.39 hours, on collagen, wild-type fibroin and RGD fibroin, respectively. * indicates significance between control and fibroin groups. *$p < 0.05$, **$p < 0.01$; by t-test. Error bars indicate square distributions; $n = 3$.

2.4. DISCUSSION

The purpose of this study was to investigate how best to quantitatively characterize cell populations in various culture conditions. The results of simulation testing showed that RFav and RFH were insensitive to the rate at which cells participated in aggregation and the number of cells involved in aggregation, respectively. However, there appeared to be a direct relationship between AD and the degree of aggregation, with increasing AD values observed for increasing cell aggregation. The significance of this relationship was confirmed statistically (Turkey-Kramer test, $p < 0.05$). Using this information, the results of the *in vitro* experiments were analyzed and the cell aggregation behavior on the different substrates analyzed. According to the time dependent changes in AD, the fibroin surface seems to be quite different from the collagen surface with respect to multicellular behavior. Promotion of cell aggregation seems to be one of characteristics of fibroin substrates, and has been reported in other studies as well (3, 5). Using observational techniques, it is easy to qualitatively

distinguish the differences between collagen and fibroin surfaces with respect to chondrocyte migration and population (Fig. 2.5 a and b). However it is quite difficult to determine whether wild-type fibroin is different from RGD fibroin in terms of cell population because this difference is too subtle to discern simply from observing photographic evidence (Fig. 2.5 b and c). In that respect, the quantitative results of this study have demonstrated that multicellular behavior is affected by the coating substrate material, and have revealed different time-dependent processes.

There are few criteria for evaluating aggregated cell populations using a Voronoi diagram so three typical sets of cell population distribution were conducted in a simulation experiment. In the aggregation distribution model, all three indexes (AD, RFav and RFH) changed according to the degree of cell density (type A), the degree of cell participation in aggregating (type B) and the number of cells in a single aggregate (type C). In types A and B, as the cells came closer each other or as the more cells became more aggregated, the cell density gap increased between crowded and barren areas, and subsequently led to an increase in AD and a decrease in RFH. Similarly, Marcelpoil et al. suggested that an increase in AD signifies populations containing aggregates in particular locations, whereas a decrease in RFH signifies populations containing barren islets (12). Moreover, Raby et al. defined the shift from initial distribution toward clustering as the increase of AD (from 0.33 to 0.57) in conjunction with the decrease of RFH (from 0.80 to 0.77) (9). In the *in vitro* experiments, AD, on average, increased significantly from 0.35 ± 0.04 to 0.55 ± 0.07 and from 0.35 ± 0.02 to 0.48 ± 0.06 for FIB and LRF substrates, respectively. On the other hand, RFH, on average, was decreased from 0.86 ± 0.032 to 0.84 ± 0.003 and from 0.88 ± 0.007 to 0.86 ± 0.002 for FIB and LRF substrates, respectively. Even though, RFH decreased for both FIB and LRF substrates, statistical significances were detected only for LRF.

There is one considerable reason why RFH did not change significantly. When less than half of the cells are in aggregation in simulation model type B, RFH values remain around 0.76, whereas RFH sensitively decreases when more than half of cells are aggregated. In addition, it seems that cell density in a cluster can also affect RFH values. Based on the results above, the RFH index varies only in the latest phase of aggregation process when a majority of cells come close to each other. On the other hand, the AD index increases gradually with cell aggregation in model types A and B. So, as far as evaluating chondrocyte aggregation on fibroin surfaces (like in Fig. 2.5), AD is more appropriate than RFH. In fact, temporal changes in AD matched well with the qualitative impressions observed experimentally.

Degree of aggregate formation has been expressed subjectively in the histomorphology

field. The AD index seems to best characterize cell-aggregate populations among the three indexes of the Voronoi Diagram under the hypotheses that positive correlation with models A (H, M, L) and B (0, 25, 50, 75, 100%) together with no correlation with model C (AGG1, AGG2, AGG3) agrees with the subjective criteria for aggregation. From time-lapse microscopy, most events in cell aggregation were observed during the first 12 hours after seeding, with cell migration subsequently normalizing, followed by cell-cell adhesion. From this analysis, chondrocyte aggregation was supposed to be a relaxation process; hence regression analysis was performed to fit the temporal AD changes recorded for each substrate into an asymptotic exponential model. As a result, the decrease in relaxation time between FIB and LRF suggests that regression analysis of AD can be used to assess whether culture substrates can affect the cell aggregation process. Interestingly, aggregation speed was delayed from 1.56 hours to 4.39 hours on the RGDSx2 peptide interfused fibroin substrate.

An RGD amino acid sequence is the minimum unit of a cell-substrate adhesive activity domain, which is a ligand of integrin (14, 15). Ryan et al. reported that decreasing substratum adhesiveness might lead to a slower rate of cell aggregation spreading over the substrate (16). Moreover, Briggs et al. reported that the weakening of cell-substrate adhesion and the formation of cell aggregates were observed simultaneously and also accompanied the osteogenic differentiation of mesenchymal stem cells (17). These results suggest that a balance between cell-cell and cell-substrate adhesion is one of the important factors in predicting cell aggregate formation/deformation. On the other hand, Kambe et al. reported that RGDSx2 peptide interfused into silk fibroin significantly increased the cell adhesive force until 12 hours after seeding (18). Taking the above into consideration, it may be possible that cell-substrate adhesiveness decreases the tendency and speed of chondrocyte aggregate formation as the adhesive force of fibroin increases.

AD analysis may be able to evaluate the motility of cellular aggregates, especially with respect to speed, which is not measured in qualitative observation. However, there are many hurdles that still remain to be cleared before this method is ready for use in tissue engineering. One of the most important problems that need to be addressed is how to translate multicellular behavior indices into design criteria for biological tissue growth. Certainly, the mechanisms underling regeneration processes are regulated by not only by cytoskeletal mediated force transmission factors, such as integrin and cadherin, but also by a network of genetic or biochemical signaling pathways. For fibroin scaffold design, it is still unclear how the chondrocyte aggregation process affects the maintenance of the cartilaginous phenotype during tissue regeneration; hence genetical or histological surveys are needed in future studies. Moreover, cell aggregation must be assessed carefully, because cell motility and

cohesion are phenomena that are central to cell organization within tissue scaffolds. Lauffenburger et al. stated that maximally useful engineering design principles for cell organization within tissue structures will require the most comprehensive models for cell motility behavior to be able to predict multicellular organization from quantifiable characteristics of cell-matrix and cell-cell interactions (19). In this respect, AD is an unrefined but easy-to-use tool for characterizing cell aggregation, and can be one of the approaches used to investigate spatio temporal characteristics of cell-matrix and cell-cell interactions.

2.5. CONCLUSION

The findings obtained from this study are the following: (1) Three indexes (the average of round factor; RFav, round factor homogeneity; RFH, and area disorder; AD) of the Voronoi diagram identified the differences in spatio-temporal changes between chondrocytes grown on fibroin and collagen surfaces; (2) The regression analysis of the AD index revealed the speed of cells during aggregation; and (3) Transgenic RGDS sequences reduced the aggregate formation of chondrocytes cultured on fibroin.

2.6. REFERENCES

1. Terryn, C., A. Bonnomet, J. Cutrona, C. Coraux, J.-M. Tournier, et al. 2009. Video-microscopic imaging of cell spatio-temporal dispersion and migration. Crit. Rev. Oncol. Hematol. 69: 144–52.

2. Liu, W.F., and C.S. Chen. 2007. Cellular and multicellular form and function. Adv. Drug Deliv. Rev. 59: 1319–28.

3. Kawakami, M., N. Tomita, Y. Shimada, K. Yamamoto, Y. Tamada, et al. 2011. Chondrocyte distribution and cartilage regeneration in silk fibroin sponge. Biomed. Mater. Eng. 21: 53–61.

4. Kim, M.-H., M. Kino-oka, Y. Morinaga, Y. Sawada, M. Kawase, et al. 2009. Morphological regulation and aggregate formation of rabbit chondrocytes on dendrimer-immobilized surfaces with D-glucose display. J. Biosci. Bioeng. 107: 196–205.

5. Kachi, N.D., A. Otaka, S. Sim, Y. Kuwana, Y. Tamada, et al. 2010. Observation of chondrocyte aggregate formation and internal structure on micropatterned fibroin-coated surface. Biomed. Mater. Eng. 20: 55–63.

6. Martinez Mozos, O., J. a. Bolea, J.M. Ferrandez, P.K. Ahnelt, and E. Fernandez. 2010. V-Proportion: A method based on the Voronoi diagram to study spatial relations in neuronal mosaics of the retina. Neurocomputing. 74: 418–427.

7. Minciacchi, D., R.M. Kassa, C. Del Tongo, R. Mariotti, and M. Bentivoglio. 2009. Voronoi-based spatial analysis reveals selective interneuron changes in the cortex of FALS mice. Exp. Neurol. 215: 77–86.

8. Bigras, G., R. Marcelpoil, E. Brambilla, and G. Brugal. 1996. Cellular sociology applied to neuroendocrine tumors of the lung: quantitative model of neoplastic architecture. Cytometry. 24: 74–82.

9. Nawrocki Raby, B., M. Polette, C. Gilles, C. Clavel, K. Strumane, et al. 2001. Quantitative cell dispersion analysis : new test to measure tumor cell aggressiveness. Int. J. cancer. 93: 644–652.

10. Zahm, J.M., S. Hazgui, M. Matos, A. Ben Seddik, B. Nawrocki Raby, et al. 2006. Quantitative videomicroscopic analysis of the sociologic behavior of non-invasive and invasive tumor cell lines. Cell. Mol. Biol. (Noisy-le-grand). 52: 54–60.

11. Matos, M., B.N. Raby, J.-M. Zahm, M. Polette, P. Birembaut, et al. 2002. Cell migration and proliferation are not discriminatory factors in the in vitro sociologic behavior of bronchial epithelial cell lines. Cell Motil. Cytoskeleton. 53: 53–65.

12. Marcelpoil, R., and Y. Usson. 1992. Methods for the study of cellular sociology: Voronoi diagrams and parametrization of the spatial relationships. J. Theor. Biol. 154: 359–369.

13. Tamura, T., C. Thibert, C. Royer, T. Kanda, E. Abraham, et al. 2000. Germline transformation of the silkworm Bombyx mori L. using a piggyBac transposon-derived vector. Nat. Biotechnol. 18: 81–84.

14. Aoki, H., N. Tomita, Y. Morita, K. Hattori, Y. Harada, et al. 2003. Culture of chondrocytes in fibroin-hydrogel sponge. Biomed. Mater. Eng. 13: 309–316.

15. Ruoslahti, E., and M.D. Pierschbacher. 1986. Arg-Gly-Asp: a versatile cell recognition signal. Cell. 44: 517–518.

16. Ruoslahti, E., and M.D. Pierschbacher. 1987. New perspectives in cell adhesion: RGD and integrins. Science. 238: 491–497.

17. Ryan, P.L., R.A. Foty, J. Kohn, and M.S. Steinberg. 2001. Tissue spreading on implantable substrates is a competitive outcome of cell-cell vs. cell-substratum adhesivity. Proc. Natl. Acad. Sci. U. S. A. 98: 4323–4327.

18. Briggs, T., M.D. Treiser, P.F. Holmes, J. Kohn, P.V. Moghe, et al. 2009. Osteogenic differentiation of human mesenchymal stem cells on poly (ethylene glycol)-variant biomaterials. J. Biomed. Mater. Res. Part A. 91: 975–984.

19. Kambe, Y., K. Yamamoto, K. Kojima, Y. Tamada, and N. Tomita. 2010. Effects of RGDS sequence genetically interfused in the silk fibroin light chain protein on chondrocyte adhesion and cartilage synthesis. Biomaterials. 31: 7503–7511.

Chapter 3.
Proposal of cell trajectory analysis as a tool to quantify cell aggregate formation

3.1. INTRODUCTION

Cell scaffolds have been essential components of tissue engineering. The optimal chemical and physical configurations of scaffold materials not only provide 3D space for cell attachment but also induce subsequent tissue development. A new tool for scaffold design is required to accomplish proper tissue formation.

Cell aggregates are one of important tools in the study of tissue development, permitting correlation of cell-cell interactions with cell differentiation, viability and migration, as well as subsequent tissue formation. The aggregate morphology permits re-establishment of the cell-cell contacts normally present in tissues; therefore, cell function and survival are often enhanced in cell aggregates. With regard to scaffold design, cell aggregates may also be useful in tissue engineering, enhancing the function of cell-based hybrid artificial organs or reconstituted tissue transplants.

Fibroin is one of the component proteins in silk produced by *Bombyx mori* silkworms, and have been used as a regenerative scaffold for various tissues, e.g. bone tissue and cartilage. Kawakami et al. evaluated chondrocyte distribution in fibroin sponges, and showed that chondrocytes formed cell aggregates in the sponge within 24 h after seeding and that cartilage tissue was formed later around those aggregates. This means that the initial aggregation process of chondrocytes in a fibroin sponge plays an important role in the formation of cartilage tissue. Other researchers said that round chondrocytes, which is typical of chondrocyte morphology, were observed within cell scaffolds and were entrapped in an abundant extracellular matrix. From tissue engineering viewpoint, the understanding of cell aggregation behavior is important for regulating tissue formation.

Cell migration analysis is a powerful tool and has been used in order to investigate the effect of cell's microenvironment (e.g., its matrix or cytokine) on cell motility. Hashimoto et al. measured cell migration speed using single-cell tracking technique and reported that a fibroin surface was able to enhance cell migration. Ware et al. quantified the effects of epidermal growth factor (EGF) treatment, and reported that EGF increased the path-length of cell migration and the frequency of changes in the cell direction. On the other hand, these

researches were performed under low-cell-density conditions in order to minimize any cell-cell interactions over the course of the experiment. Therefore, cell aggregation mechanisms remain yet to be clarified because of lack of quantitative method of cell aggregate formation. Hall et al. categorized cartilage formation into 4 processes: (1) cell migration, (2) intercellular contact and adhesion, (3) aggregation (condensation), and (4) cartilage differentiation. Based on this viewpoint, cell-cell distance is one of the important factors for characterizing the cell aggregation, because cell-cell contact is a triggering event of cell aggregate formation. The focus of this section is to introduce quantitative method of cell aggregate formation, in which cell-cell distance was measured using cell trajectory data. Additionally, chondrocyte motility over different substratum protein and culture medium was analyzed, and the effect of chondrocyte migration on subsequent aggregate formation was investigated. Fibroin and ProNectin were used for different substrates model, and culture medium with and without insulin-like growth factor 1 (IGF-1), which was reported to promote cell migration, were used for culture medium. Cell shape and migration speed was also evaluated, and the relationship between these two features and the results of cell aggregate quantitation was investigated using multiple regression analysis.

3.2. MATERIALS AND METHODS

Chondrocytes isolated from 4-week-old Japanese white rabbits were passaged once and seeded on culture dishes coated with substrates (Fig. 3.1) and cell behavior was observed with a phase contrast microscope for 24 h. The details are described below.

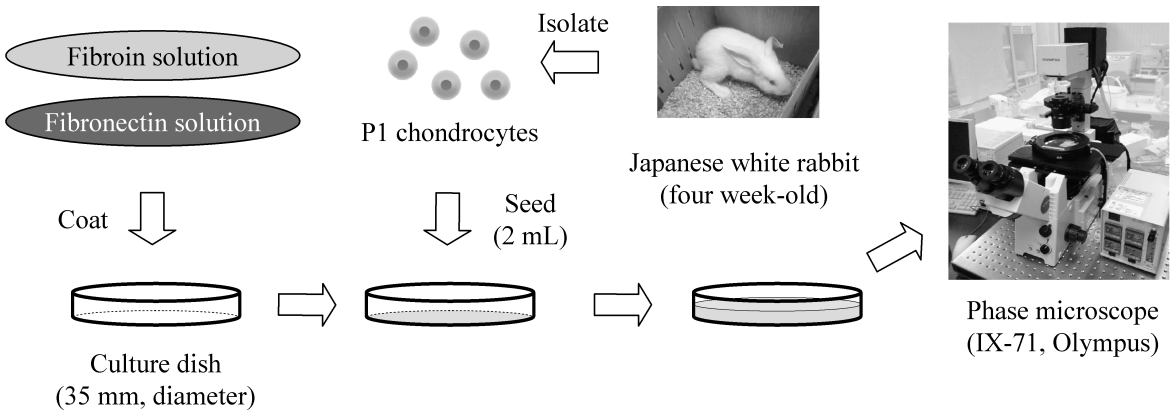

Fig. 3.1 Experimental procedures for the observation of chondrocyte behavior.

3.2.1. Substrates preparation

A fibroin aqueous solution was prepared as described previously. Briefly, degummed silk fibroin fibers of *Bombyx mori* cocoons were dissolved in 9 M lithium bromide aqueous solution at room temperature, and then the solution was dialyzed against pure water. The concentration of fibroin in the water solution was determined by colorimetric method and was prepared to be 1% (wt/vol). Before coating the fibroin substrate, culture dishes (diameter, 35 mm; Asahi Glass Co., Ltd., Japan) were washed with acetone and completely dried at 50°C. Culture dishes were soaked in fibroin solution for 1 minute at room temperature, and then dried at 50°C. The dishes were immersed in 80% methanol solution for 1 h, and dried again at 50°C. Fibroin-coated culture dishes were washed with Dulbecco's Phosphate Buffered Saline (PBS) (Nacalai Tesque, Inc., Japan) before experiments.

ProNectin is a 75 kD protein polymer genetically engineered using a repeated peptide segment of GAGAGS originating from fibroin, and using a cell attachment epitope containing the Arg-Gly-Asp (RGD) peptide sequence from fibronectin. An RGD sequence is the minimum unit of the cell–substrate adhesive activity ligand, and alters cell fate through integrin-mediated binding. Therefore, to create a non-aggregating control group, protein coated plates were prepared using ProNectin F (Sigma-Aldrich Corp., USA) according to the manufacturer's instructions. Briefly, stock solution was diluted to 10 μg/mL in PBS. Culture dishes were then soaked in the diluted solution for 5 min at room temperature. Afterwards, the culture dishes were washed twice with PBS.

3.2.2. Chondrocytes preparation

Chondrocytes were prepared as described previously. Briefly, articular cartilage tissue samples were aseptically harvested from the humeri, femora, and tibias of 4-week-old male Japanese white rabbits (Oriental Bio Service, Japan). The cartilage samples were enzymatically digested, and chondrocytes isolated using a Cell Strainer (BD Biosciences, USA) were washed twice with PBS and preserved at -80°C until examination.

Cells were passaged once prior to experimentation for 5 days in tissue culture flask (25 cm^2, Asahi Glass Co., Ltd., Japan.) They were incubated at 37°C in a humidified atmosphere of 95% air and 5% CO_2. The culture medium was Dulbecco's Modified Eagle Medium (DMEM; Nacalai Tesque, Japan) containing 10 vol% Fetal Bovine Serum (Nacalai Tesque, Japan), and 1 vol% antibiotic mixture (10,000 units/mL penicillin, 10 mg/mL streptomycin, and 25 μg/mL amphotericin B; Nacalai Tesque, Japan) and was changed on day 3.

3.2.3. Time-lapse observation

Chondrocytes were removed from the flask by adding 0.25% trypsin-EDTA to the culture medium on day 5. The recovered cell suspension (concentration, 1.0×10^4 cells/cm^2) in Leibovitz's L-15 medium (Invitrogen Corp., USA) containing 10 vol% Fetal Bovine Serum, and 1 vol% antibiotic mixture was seeded to substrate-coated culture dishes. Recombinant Human IGF-1 (R&D Systems, Inc., USA) was added to the cell suspension of the IGF+ group at a concentration of 10 ng/mL before seeding.

Chondrocyte migration was observed by time-lapse microscopy using a phase-contrast microscope (IX-71, Olympus Corp., Japan). During observation, cells were incubated at 37°C in a humidified atmosphere in a culture chamber (MI-IBC-IF; Olympus, Japan). During a 24-h culture period, time-lapse phase contrast images were captured every 10 minutes by a CCD camera (DP70; Olympus, Japan). Three movies were captured for fibroin+, fibroin-, ProNectin+ and ProNectin- group, respectively.

Every cell captured during the time-lapse observation was manually tracked using MTrackJ, an ImageJ (National Institutes of Health, MD) tracking plugin. Position data for all the cells was measured by the MTrackJ tracking function and was recorded in spreadsheets to calculate the distances between each pair of cells and to quantify cell distribution.

3.2.4. Analysis of cell shape

Cells for which pseudopodia were observed were defined as elongated cells, while the other cells were defined as round cells. Analysis was performed for each photo, and each cell was re-categorized every time.

3.2.5. Analysis of migration speed

The migration speed of each cell was calculated using the positional information of obtained by MTrackJ. In order to obtain as reliable data as possible, the cells that were at the edge of the field of view and that divided were excluded from analysis objects.

3.2.6. Analysis of cell aggregate formation

Based on the position of each cell, the degree of aggregation was analyzed using Moving-Node Grouping Method (MNGM), a quantitative method to evaluate cell aggregation behavior. Figure 2 is the conceptual diagram of this assay. Each cell is considered a moving node, and MNGM collects the information on intercellular interaction

such as contact and adhesion, depending on intercellular distance. Specifically, if 2 cells were less than 40 μm apart, the condition was defined as intercellular contact. If the cells remain to contact with each other for more than 1 h, the condition was defined as intercellular adhesion. A group of cells that adhered to each other was defined as an aggregate. The rate that the cells joined an aggregate was defined as aggregation rate. Intercellular Contact Index (*ICI*), the frequency of intercellular contacts normalized with the number of cells, was defined as follows: $ICI = n_c / {}_nC_2$, where n represents the number of cells, and n_c represents the number of intercellular contacts.

The status of cellular shape, migration speed, and aggregation rate varies from hour to hour. As such, averages for the percentage of round cells and migration speed during the culture period, along with the aggregation rate at 24 h after seeding were used for analysis.

3.2.7. Statistical analysis

Values among the 4 groups were compared using ANOVA and Tukey's test for post hoc comparison. Multiple regression analysis was performed in order to quantitatively investigate the relationship between the percentage of round cells, migration speed, and aggregation rate. All statistical tests were two-tailed analyses with significance at $p < 0.05$.

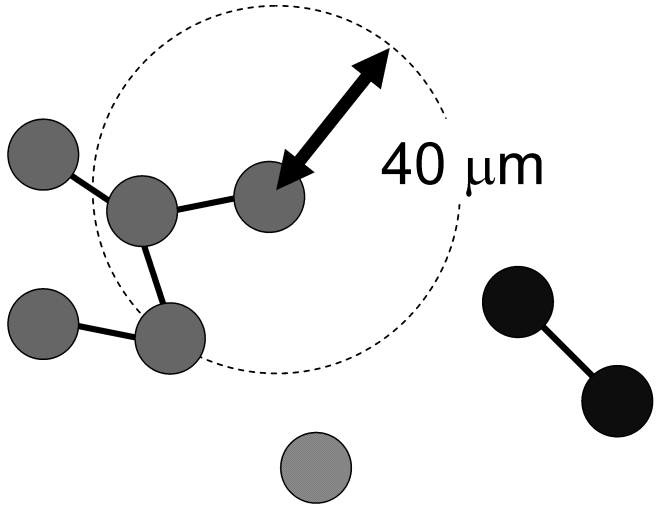

Fig. 3.2 Conceptual diagram of Biological Node Grouping Method. Adjacent cells whose distance is less than 40 mm are connected with line, and these cells are defined to be an aggregate.

3.3. RESULTS

Figure 3 shows the percentage of round cells, where the fibroin groups showed significantly higher values than those for the ProNectin groups. There was no significant difference caused by the addition of IGF-1.

The average migration speed of the fibroin IFG– group showed significantly higher value than those for the other 3 groups, and the migration speed for the fibroin_IGF+ group migrated significantly faster than that for the ProNectin IFG– group (Fig. 4).

The aggregation rate at 24 h after seeding is shown in Fig. 5. Though there was no significant difference between the 4 groups, the fibroin groups tended to have higher aggregation rates than the ProNectin groups.

Table 1 shows the results of multiple linear regression analysis. The relationship calculated between aggregation rate G, the percentage of round cells ρ_R, and migration speed S was $G = 25.9 - 0.0584\rho_R + 0.674S$. Correlation matrix was shown in Table 2. There was no statistically significant correlation between the percentage of round cells and aggregation rate ($p > 0.05$, $r = 0.340$), while there was statistically significant positive correlation between migration speed and aggregation rate ($p < 0.05$, $r = 0.689$).

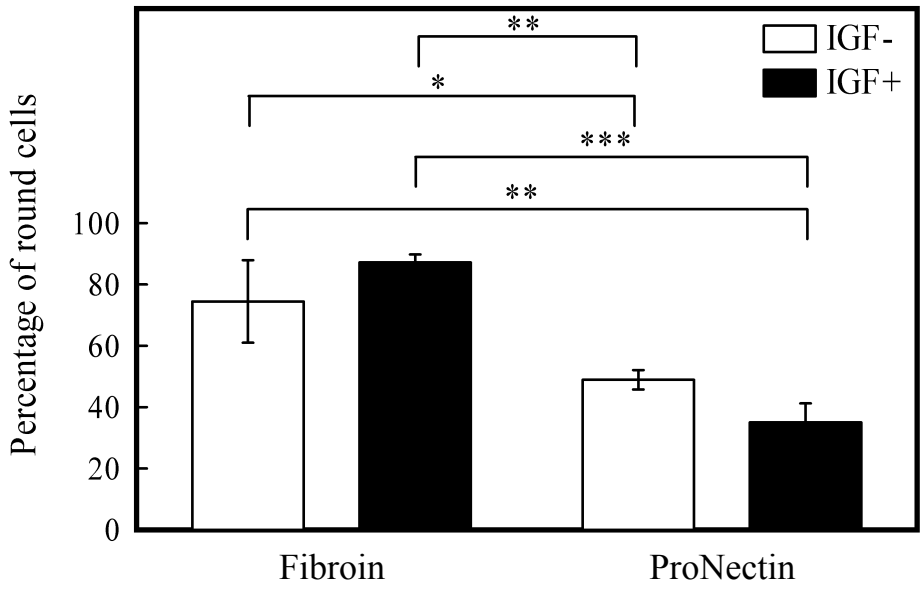

Fig. 3.3 Percentage of round cells. The values of fibroin groups were significantly higher than those of ProNectin groups. (n = 3, the number of analyzed cells = 259 ± 68, *: $p < 0.05$, **: $p < 0.01$, ***: $p < 0.001$)

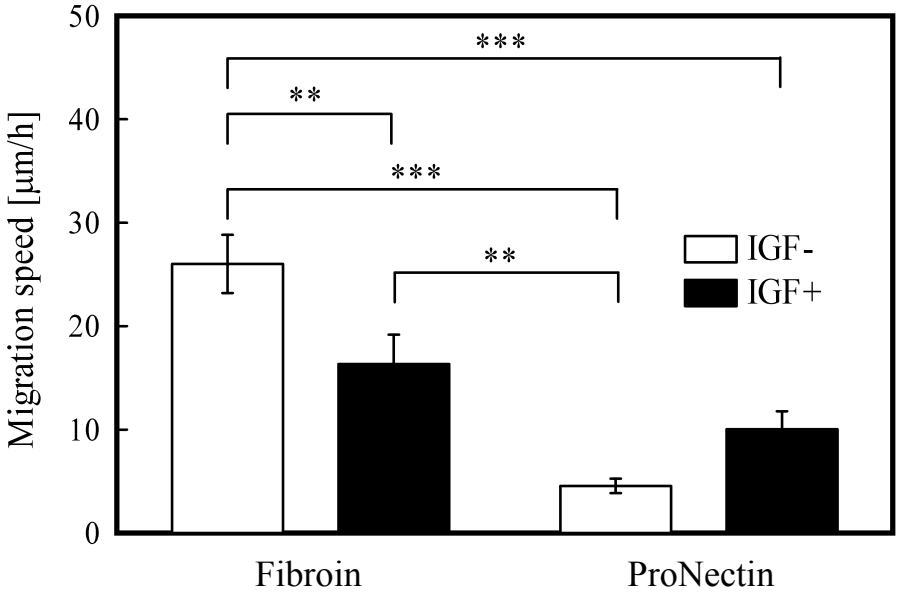

Fig. 3.4 Average migration speed. Fibroin_IGF- group migrated significantly faster than the other 3 groups, and Fibroin_IGF+ group migrated significantly faster than ProNectin_IGF- group. (n = 3, the number of analyzed cells = 181 ± 57, **: $p < 0.01$, ***: $p < 0.001$)

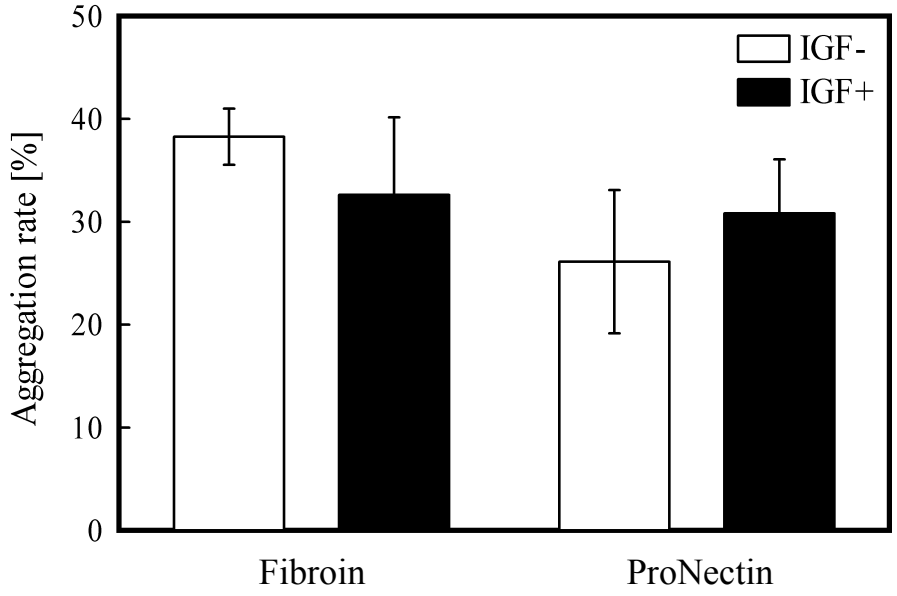

Fig. 3.5 Aggregation rate at 24 h after seeding. Though there was not significant difference among 4 groups, the fiborin groups tended to have higher values than the ProNectin groups. (n = 3, the number of analyzed cells = 280 ± 76)

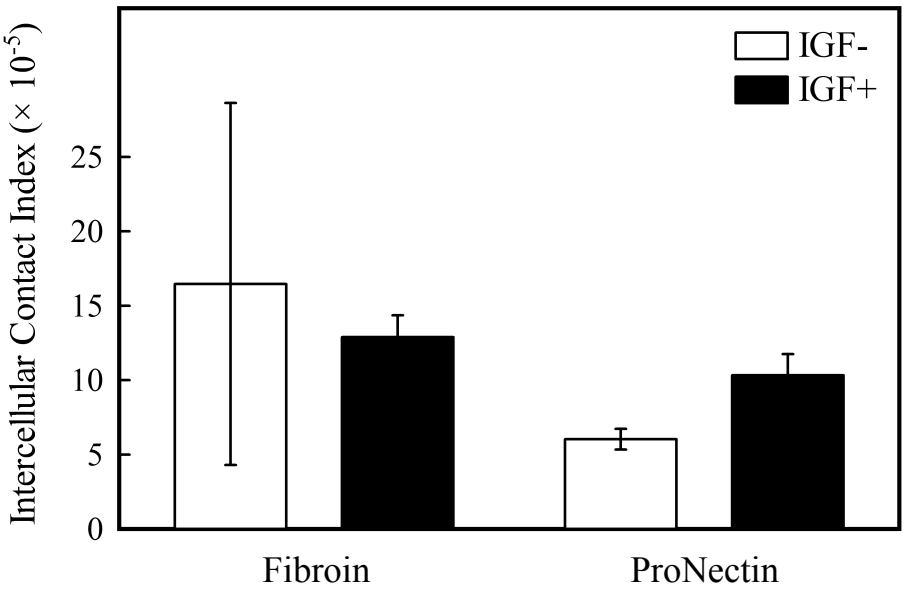

Fig. 3.6 Intercellular Contact Index, the frequency of intercellular contacts normalized with the number of cells. Though there was no significant difference among the 4 groups, the WTF groups tended to have higher values than those for the FN groups. (n = 3, the number of analyzed cells = 259 ± 68)

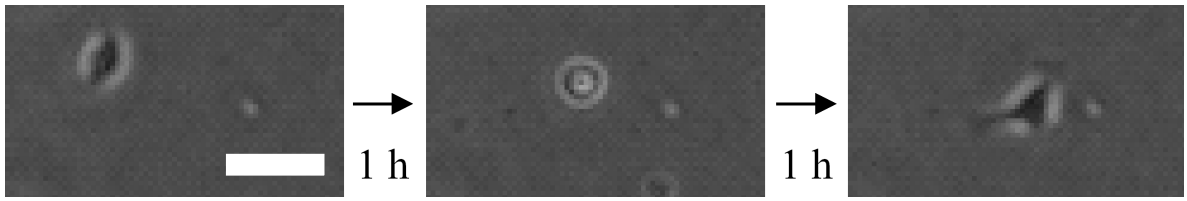

Fig. 3.7 Morphological changes of a chondrocyte on a fibroin substrate.
However, on fibronectin substrates, once cells got elongated, most cells did not undergo a morphological change into round shape. Scale bar, 100 mm.

TABLE 1. Results of multiple regression analysis.
(*: $p < 0.05$, ***: $p < 0.001$)

	Regression coefficient
Intercept	25.9 (***)
Percentage of round cells	-0.0584
Migration speed	0.674 (*)
R (Multiple Correlation Coefficient)	0.703 (*)
R^2 (Coefficient of Determination)	0.495

TABLE 2. Correlation matrix

	Percentage of round cells	Migration speed	Aggregation rate
Percentage of round cells	1.000		
Migration speed	0.647	1.000	
Aggregation rate	0.340	0.689	1.000

3.4. DISCUSSION

Scaffold design has been performed using multidisciplinary research such as on mechanical strength, porosity, space for nutrient supply, and so on. However, the trial to explore every possibility at once significantly increases the complexity of the design problem. The purpose of this paper is to refine the variables to design extracellular environments that facilitate chondrocyte aggregate formation under the hypothesis that the cell aggregation played an important role for better cartilage-tissue formation. The results showed statistically significant positive correlation between migration speed and aggregation rate. Though *ICI*s was no significant difference among the 4 groups, the fibroin groups tended to have higher values than those for the ProNectin groups (Fig. 6). Migration speed was found to correlate with the frequency of intercellular contact ($r = 0.696$). Considering the aggregation process, i.e. cell migration, and intercellular contact and adhesion, high migration speed possibly led to an increase in the frequency of intercellular contact, and the subsequent high aggregation rate. The results in Table 1 and 2 suggest that a culture environment that allows cells to easily migrate on the surface of scaffold could be effective in cartilage tissue formation. For example, modification of material properties (e.g. dendrimer surface), the introduction of adhesive ligands to the material (e.g. RGD motif), and the addition of growth factor (e.g. IGF-1 and bFGF), all of which have been reported to promote chondrocyte migration, could be useful for cartilage tissue engineering in the future.

This study showed contradictory data that the addition of IGF-1 decreased the migration speed on fibroin substrates while it increased the migration speed on fibronectin substrates. However, this fact can be explained as follows. It has been reported that IGF-1 increases the production of proteoglycan. It has also reported that proteoglycan inhibits the adhesion of chondrocytes to substrates. DiMilla et al. reported that the relationship between migration speed and cell–substrate adhesion of smooth muscle cells was not linear but had a peak, and it has been shown that the intermediate level of adhesion strength induces cell migration the most. Considering the similar relationship for chondrocytes, if the adhesion of the ProNectin group was relatively strong and that of fibroin group was relatively weak than the peak value, it would be possible that the addition of IGF-1 affected the migration speed in this way.

There was no significant correlation between the percentage of round cells and aggregation rate, i.e. the result suggests that cellular shape ratio does not have a great effect on aggregation. However, this study analyzed a whole cell group statistically, not the migratory behavior of each cell. Focusing on each cell's motion, repeated morphological

changes of a chondrocyte were observed on a fibroin substrate (Fig. 7). On the other hand, on fibronectin substrates, once cells got elongated, most cells did not undergo a morphological change into round shape. Kim et al. reported that chondrocyte underwent intermittently morphological changes on dendrimer-immobilized glucose substrate and that chondrocytes formed aggregates later on that substrate. Considering these results, frequent changes of cellular morphology could play an important role in subsequent aggregate formation. Further study to investigate the effects of cellular shape on aggregation is required to understand the role of extracellular environment in cartilage differentiation.

In conclusion, our observation of cell migration suggests that achieving high migration speed could be effective to promote chondrocyte aggregate formation. The effects of cellular shape on aggregation and formed aggregates need to be investigated further.

3.5. REFERENCE

1. Kim, B.S., and Mooney, D.J. Development of biocompatible synthetic extracellular matrices for tissue engineering. Trends Biotechnol **16**, 224, 1998.

2. Hutmacher, D.W. Scaffold design and fabrication technologies for engineering tissues—state of the art and future perspectives. J Biomater Sci Polym Ed **12**, 107, 2001.

3. Chen, G., Ushida, T., and Tateishi, T. Scaffold Design for Tissue Engineering. Macromol Biosci **2**, 67, 2002.

4. Hollister, S.J. Porous scaffold design for tissue engineering. Nat Mater **4**, 518, 2005.

5. Owen, S.C., and Shoichet, M.S. Design of three-dimensional biomimetic scaffolds. J Biomed Mater Res A **94A**, 1321, 2010.

6. Tomita, N. Bio-environment designing for biomaterials (in Japanese). Journal of Society of Materials Science, Japan **53**, 91, 2004.

7. Hall, B.K, and Miyake, T. All for one and one for all: condensations and initiation of skeletal development. Bioessays **22**, 138, 2000.

8. DeLise, A.M., Fischer, L., and Tuan, R.S. Cellular interactions and signaling in cartilage development. Osteoarthritis Cartilage **8**, 309, 2000.

9. Kawakami, M., Tomita, N., Shimada, Y., Yamamoto, K., Tamada, Y., Kachi, N., and

Suguro, T. Chondrocyte distribution and cartilage regeneration in silk fibroin sponge. Biomed Mater Eng **21**, 53, 2011.

10. Aoki, H., Tomita, N., Morita, Y., Hattori, K., Harada, Y., Sonobe, M., Wakitani, S., and Tamada, Y. Culture of chondrocytes in fibroin-hydrogel sponge. Biomed Mater Eng **13**, 309, 2003.
11. Kachi, N., Tomita, N., Yamamoto, K., Takaya, R., and Tamada, Y. Tribological maturation of regenerated cartilage was inhibited by using chondrocyte aggregates. Journal of Biomechanical Science and Engineering **4**, 174, 2009.
12. Kachi, N.D., Otaka, A., Sim, S., Kuwana, Y., Tamada, Y., Sunaga, J., Adachi, T., and Tomita, N. Observation of chondrocyte aggregate formation and internal structure on micropatterned fibroin-coated surface. Biomed Mater Eng **20**, 55, 2010.
13. Otaka, A., Kachi, N.D., Takeda, Y., Sim, S., Tomita, N., Kuwana, Y., and Tamada, Y. Study of cellular sociology applied to cartilage regeneration. Abstract presented at SSI2010, Kyoto, Japan, 2010.
14. Otaka, A., Shimada, Y., Kawakami, M., Kachi, N.D., Yamamoto, K., Tamada, Y., Suguro, T., and Tomita, N. Quantitative evaluation of cell aggregating process at early stage of cartilage regeneration. Abstract presented at 56th Annual Meeting of ORS, New

Orleans, LA, 2010.

15. Chang, M.E., Lauffenburger, D.A., and Morales, T.I. Motile chondrocytes from newborn calf: migration properties and synthesis of collagen II. Osteoarthritis Cartilage **11**, 603, 2003.

16. Luyten, F.P., Hascall, V.C., Nissley, S.P., Morales, T.I., Reddi, A.H. Insulin-like growth factors maintain steady-state metabolism of proteoglycans in bovine articular cartilage explants. Arch Biochem Biophys **267**, 416, 1988.

17. Schmidt, M.B., Chen, E.H., and Lynch, S.E. A review of the effects of insulin-like growth factor and platelet derived growth factor on *in vivo* cartilage healing and repair. Osteoarthritis Cartilage **14**, 403, 2006.

18. Takeda, Y., Otaka, A., Tamada, Y., and Tomita, N. Quantification of the relationship between cell shape and intercellular adhesion of chondrocytes on a fibroin substrate. Abstract presented at the 23rd European Conference on Biomaterials, Tampere, Finland, 2010.

19. Meijering, E. MTrackJ. http://www.imagescience.org/meijering/software/mtrackj/.

20. Kim, M.H., Kino-oka, M., Morinaga, Y., Sawada, Y., Kawase, M., Yagi, K., and Taya, M. Morphological regulation and aggregate formation of rabbit chondrocytes on

dendrimer-immobilized surfaces with D-glucose display. J Biosci Bioeng **107**, 196, 2009.

21. Connelly, J.T., Garcia, A.J., and Levenston, M.E. Interactions between integrin ligand density and cytoskeletal integrity regulate BMSC chondrogenesis. J Cell Physiol **217**, 145, 2008.

22. Maniwa, S., Ochi, M., Motomura, T., Nishikori, T., Chen, J., and Naora, H. Effects of hyaluronic acid and basic fibroblast growth factor on motility of chondrocytes and synovial cells in culture. Acta Orthop Scand **72**, 299, 2001.

23. Van Osch, G.J., van den Berg, W.B., Hunziker, E.B., and Häuselmann, H.J. Differential effects of IGF-1 and TGF beta-2 on the assembly of proteoglycans in pericellular and territorial matrix by cultured bovine articular chondrocytes. Osteoarthritis Cartilage **6**, 187, 1998.

24. Imoto, E., Kakuta, S., Hori, M., Yagami, K., and Nagumo, M. Adhesion of a chondrocytic cell line (USAC) to fibronectin and its regulation by proteoglycan. J Oral Pathol Med **31**, 35, 2001.

25. Yamagata, M., Suzuki, S., Akiyama, S.K., Yamada, K.M., and Kimata, K. Regulation of Cell-Substrate Adhesion by Proteoglycans Immobilized on Extracellular Substrates. J Biol Chem **264**, 8012, 1989.

26. DiMilla, P.A., Stone, J.A., Quin, J.A., Albelda, S.M., and Lauffenburger, D.A. Maximal Migration of Human Smooth Muscle Cells on Fibronectin and Type IV Collagen Occurs at an Intermediate Attachment Strength. J Cell Biol **122**, 729, 1993.

27. Huttenlocher, A., Sandborg, R.R., and Horwitz A.F. Adhesion in cell migration. Current Opinion in Cell Biology **7**, 697, 1995.

Chapter 4.
Quantification of cell co-migration occurrences during cell aggregation on fibroin substrates

4.1. INTRODUCTION

Cell migration within a three-dimensional matrix or over a two-dimensional substrate occurs in a wide variety of physiological and biotechnological situations, such as tissue repair, immune response reactions, and tumor invasion (1). Various stimuli from the surrounding environment influence how the cells behave, and determine whether events such as differentiation and aggregation take place. For example, changes in cell-cell adhesion may initiate cell migration, while cell-substrate adhesion has been shown to regulate cell migration behavior. As a result, the effects of substrate mechanics on cell behavior have been under intense investigation.

Fibroin is one of the component proteins in silk produced by *Bombyx mori* silkworms, and is widely used in biomedical applications (2). Moreover, in the field of tissue engineering, many researchers have investigated fibroin's ability to be used as a regenerative scaffold for various tissues, such as bone tissue (3,4) and cartilage (5–7). Kawakami et al. used fibroin sponges as scaffolds for chondrocyte cultivation and demonstrated that initial chondrocyte aggregation in fibroin sponges led to enhanced cartilage tissue formation (7). Additionally, in chapter 2 and 3, the collective behavior of cells on fibroin substrates was investigated, and it was observed that fibroin was able to both enhance cell-cell interactions during cultivation and control the speed of cell aggregation behavior during cell migration (8). From both scientific and engineering viewpoints, the understanding of cell-cell and cell-substrate interactions is important for clarifying and regulating cell aggregation and subsequent tissue formation. However the mechanisms by which matrices (e.g. fibroin) influence events such as cell aggregation remain yet to be clarified.

Cell aggregation has been observed in many studies (8–12), but a number of these studies have been qualitative and highly researcher dependent. A few studies, however, have been successful in applying quantitative evaluation methods to cell behavior analysis (8,10,13). In chapter 2, the authors evaluated chondrocyte aggregation on fibroin substrates using Voronoi diagram analysis (8), which proved to be successful in identifying global cell aggregation behavior. However, the Voronoi diagram technique was insufficient for evaluating the

specific behavior of individual cells during aggregation, because the technique focuses on the overall spatial distribution of cells rather than individual cell behavior during aggregate formation. In mass animal locomotion studies, i.e. schools of fish or flocking birds, many researchers have focused on the distances between neighboring members to both evaluate and recreate observed behavior (14). Therefore, cell-cell distance and its dynamic changes may be useful for characterizing the cell aggregation process. By understanding the distance over which cells interact with adjacent cells, it may be possible to gain insights into the mechanisms of cell aggregation. In this chapter, chondrocyte behavior on fibroin substrates was quantitatively evaluated by focusing on the distances between neighboring cells. Specifically, the motion of cell pairs that maintained an intercellular distance of D μm, termed co-migration, was evaluated.

4.2. MATERIALS AND METHODS

The motion of cell pairs maintaining an intercellular distance of D μm, which we have termed co-migration, was recorded and analyzed for various threshold distances (D). To define a range of D values, the major diameters of a random sample of cells were measured, as cell size can affect the cell-cell distance when two cells are in contact with each other. Then, to verify co-migration as a method for evaluating cell aggregation behavior, cell distribution analysis was performed using the previously validated Voronoi diagram approach. The results of the co-migration analysis and the results of the Voronoi diagram analysis were then compared using correlation analysis, and values of D that demonstrated good correlation were identified. Using these criteria, the chondrocyte aggregation behavior on fibroin substrates was investigated in detail with respect to the rate of cells participating in co-migration and the time over which cell co-migration occurred.

4.2.1. Cell preparation

Chondrocytes were aseptically harvested from the proximal humerus, distal femur, and proximal tibia of 4-week-old Japanese White rabbits (Oriental Bio Service, Japan), and passaged once prior to experimentation, as described previously (8).

4.2.2. Substrate plate preparation

To create fibroin coated plates, a fibroin aqueous solution was prepared as described previously. Briefly, degummed silk fibroin fibers of *Bombyx mori* cocoons were dissolved in 9 M lithium bromide aqueous solution at room temperature, and then the solution was

dialyzed against pure water. The concentration of fibroin in the water solution was determined by colorimetric method and was prepared to be 1% (wt/vol). Before coating the fibroin substrate, 35 mm glass bottom dishes (Asahi Techno Glass, Japan) were washed with acetone and completely dried at 50°C. Culture dishes were soaked in fibroin solution for 1 min at room temperature, and then dried at 50°C. The dishes were immersed in 80% methanol solution for 1 h, and dried again at 50°C.

ProNectin is a 75 kD protein polymer genetically engineered using a repeated peptide segment of GAGAGS originating from fibroin, and using a cell attachment epitope containing the RGD peptide sequence from fibronectin (15,16). An RGD sequence is the minimum unit of the cell–substrate adhesive activity ligand, and alters cell fate through integrin-mediated binding. Therefore, to create a non-aggregating control group, protein coated plates were prepared using ProNectin F (Sanyo Chemical Industries, Japan) according to the manufacturer's instructions. Briefly, stock solution was diluted to 10 μg/mL in PBS. Culture dishes were then soaked in the diluted solution for 5 min at room temperature. Afterwards, the culture dishes were washed twice with PBS.

4.2.3. Time-lapse observation and cell trajectory acquisition

Passaged chondrocytes were suspended in Leibovitz's L-15 medium (Invitrogen, CA) containing 10 vol% fetal bovine serum (Nichirei Biosciences Inc., Japan), 1 vol% antibiotic mixture (Nacalai Tesque, Japan) and 0.2 mM ascorbic acid (A8960; Sigma-Aldrich Japan, Japan), and 1.0×10^5 cells were seeded in 2 mL of cell suspension medium at a concentration of 5.0×10^4 cells/mL (approximately 1×10^4 cells/cm^2).

Each dish was enclosed in a culture chamber (MI-IBC-IF; Olympus, Japan) in a humidified atmosphere at 37°C and placed on an inverted phase contrast microscope (IX-81; Olympus, Japan). During a 24-h culture period, time-lapse phase contrast images were captured every 10 minutes by a CCD camera (DP70; Olympus, Japan). Five movies were captured for the respective fibroin and ProNectin groups.

Every cell captured during the time-lapse observation was manually tracked using MTrackJ, an ImageJ (National Institutes of Health, MD) tracking plugin (17). Position data for all the cells was measured by the MTrackJ tracking function and was recorded in spreadsheets to calculate the distances between each pair of cells and to quantify cell distribution.

4.2.4. Measurement of cell size and circularity

Cell diameters and circularity were evaluated by using ImageJ. Cells on each substrate were randomly chosen with respect to culture time and cell location and each cell's profile was outlined manually. Subsequently, the major diameters of each outline (maximum Feret's diameters) were measured (n = 25; for each movie). The maximum Feret's diameter, also known as the maximum caliper diameter, is the longest distance between 2 points on an object (18). Cell circularity was measured using the formula $4p(\text{area}/\text{perimeter}^2)$. A circularity value of 1 indicates a perfect circle, while a circularity value approaching 0 indicates an increasingly elongated polygon.

4.2.5. Cell distribution quantitation

A geometrical model based on a Voronoi tessellation, derived by Marcelpoil et al. (19), was used to characterize spatiotemporal changes in the chondrocyte aggregation behavior. According to cell position information, each snapshot image was partitioned into N regions (Voronoi cells), where N was the number of cells in sight. The disorder of the Voronoi cell area (area disorder) was calculated using the equations of Marcelpoil et al. (19). In chapter 2, increasing area disorder values were observed for increasing chondrocyte aggregation on fibroin substrates (8).

4.2.6. Evaluation of cells participating in co-migration

Co-migration rate was then evaluated by measuring the Euclidean distances between cells, and cells located less than a threshold distance D apart were recorded using R (The R Foundation for Statistical Computing, Austria). A grouping assay of moving objects was performed (see Appendix), and the rates at which the cells participated in co-migration were calculated.

Then in order to clarify which cell-cell distance was appropriate for characterizing aggregation behavior, the association between Voronoi diagram analysis and the rate of cells participating in co-migration (co-migration rate) was investigated, and the values of D that showed good correlation were identified.

4.2.7. Evaluation of rate of cells participating in co-migration and aggregation behavior

To look at the differences between cell aggregation behavior on fibroin and ProNectin

substrates, the co-migration rates on each substrate were evaluated with respect to various threshold time values (*T*). ProNectin substrates were used as a non-aggregating control group, and the average of the co-migration rates for each substrate were compared.

4.2.8. Evaluation of time over which cell co-migration occurred

Focusing on the time over which cell co-migration occurred, the stability of the cell-cell contacts on each substrate was evaluated. In practice, some cells moved into/out of frame during the time-lapse observation, leading to a reduction in accuracy. Therefore, the Kaplan–Meier estimator was used, and out of frame cell data was referred to as censored data. In addition, cell pairs that emerged simultaneously because of frame entrance or mitotic divisions were excluded in this analysis.

4.2.9. Statistical tests

The Kaplan–Meier estimator was used to calculate the survival function for cell co-migration data for the fibroin and ProNectin groups, and a statistical comparison of the survival function was done using the log-rank test. The difference between cell diameter or circularity on fibroin and ProNectin was analyzed using the Mann-Whitney test. All tests were performed with a significance level of 0.05.

4.3. RESULTS

4.3.1. Formation of cells with a rounded shape on fibroin substrates

Fig. 4.1 shows chondrocyte images during cultivation. On the ProNectin substrate, most of the cells were elongated, and few cells were found to be in contact with each other. On the fibroin substrate, however, many chondrocytes maintained a rounded shape and participated in cell aggregation. The average cell number observed on fibroin and ProNectin substrates ranged from 79–155 and 80–157 cells per frame, respectively. There was no significant difference in cell density observed between on fibroin and ProNectin substrates.

The recorded major diameters of the cells are shown in Fig. 4.2. On fibroin substrates, the major diameters of the cells ranged from 11.7–107.7 μm. On the other hand, in the ProNectin group, major diameter values (range: 12.1–124.3 μm) were larger than those on the fibroin substrates. In addition, the cell circularity increased with decreasing major diameter. On fibroin substrates, many cells were less than 20 μm in diameter, and the peaks for cell

diameter were located in the range of 10–20 μm, which seemed to indicate a rounded cell shape. The major diameters of 90% of the cells were smaller than 59.0 μm on the fibroin substrates, and smaller than 72.0 μm on the ProNectin substrates.

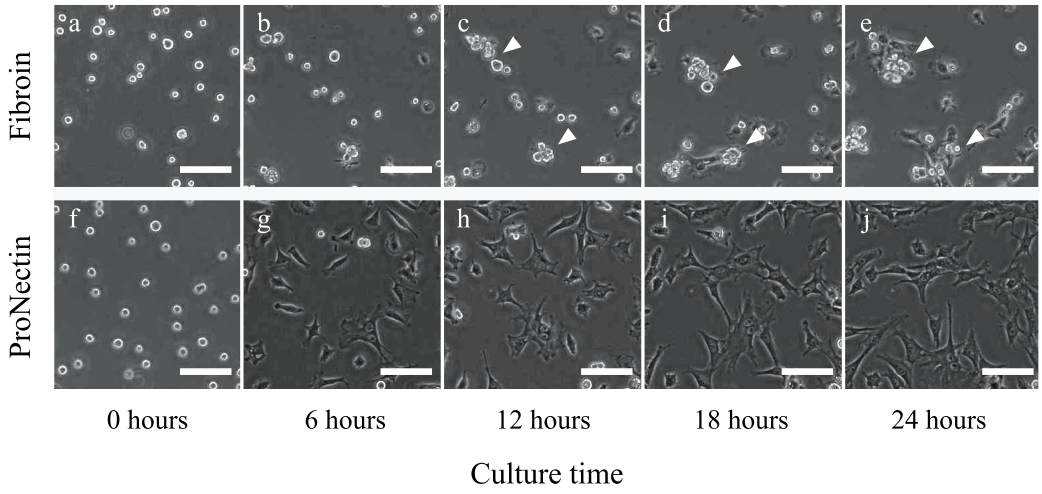

Fig. 4.1 Phase contrast images of chondrocytes cultured on wild-type fibroin (a), and on ProNectin (b), which were taken 0, 6, 12, 18 and 24 h after seeding. Round shaped cells formed cell aggregations on the fibroin substrate. Cell aggregation changes moved according during cultivation (white arrows). Scale bar = 100 μm.

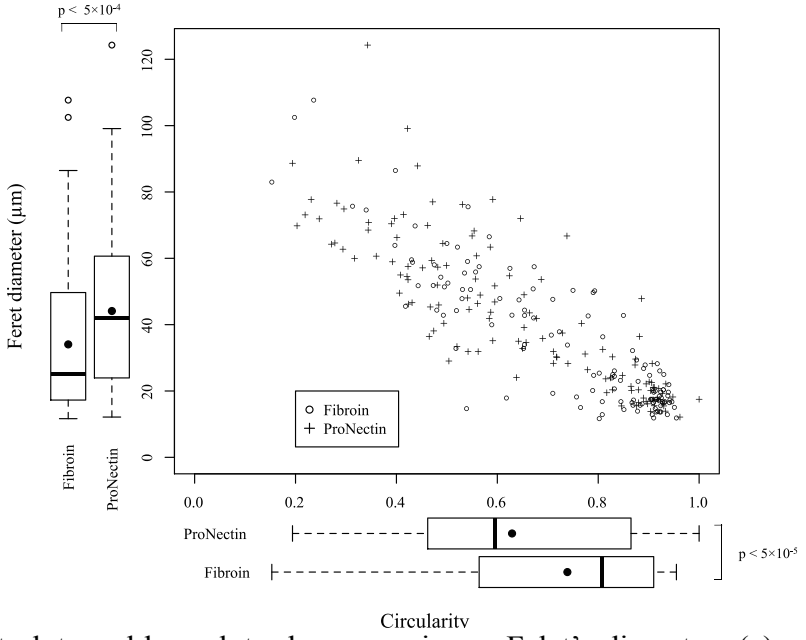

Fig. 4.2 Dot plots and box plots shows maximum Felet's diameters (a) and minimum Felet's diameters (b) of cells on each substrate. Dots and horizontal lines in boxes indicate the mean and median of the diameters, respectively. There was a peak in 20 mm in the density function of cell diameter on fibroin substrates. (n = 125 for each group; 25 cells per video)

4.3.2. Correlation between Voronoi diagram analysis and cell-cell distance evaluation

A Voronoi diagram cell aggregation assay was performed, and the area disorder value, which represents the degree of cell aggregation, was compared with the cell co-migration rates as measured by various threshold times *T* and threshold distances *D*. Fig. 4.3*a* shows the time-dependent changes in area disorder for chondrocytes grown on each substrate. The area disorder values in the ProNectin group showed little change over 24 h. However, the area disorder values for the fibroin group gradually increased in a time dependent manner. Looking at the standard deviations from Fig. 4.3, the degree of cell aggregation varies widely in response to the observation location.

Fig. 4.3*b* shows an example of the time-dependent changes in the co-migration rate (calculated for $D = 40$ μm and $T = 110$ minutes). Fig. 4.4 shows the results of the correlation coefficients for a different (*D*, *T*) threshold set. The correlation coefficient (range: -1.0–1.0) was used to measure how well the co-migration rate agreed with the cell aggregation rate (as measured by area disorder), with values close to 1 indicating good agreement. In the fibroin group, the correlation coefficients ranged from -0.05–0.76, and a high value of correlation between the area disorder and the co-migration rate (more than 0.7) was observed for low *D* and *T* conditions (range: 22–58 μm and 0.16–6.50 h, respectively) In contrast, high correlation values were not observed on the ProNectin substrate (range: -0.46–0.54). Moreover, the highest correlation value between the co-migration analysis and the Voronoi diagram analysis was observed for $T = 110$ minutes. From these results, the *T* value (hereafter, 110 minutes) was used for evaluating cell co-migration rates (in Fig. 4.5) and measuring survival rate for co-migration (in Fig. 4.7).

4.3.3. The differences in cell co-migration between the fibroin and ProNectin groups

The average rate at which chondrocytes formed aggregates on the fibroin and ProNectin substrates was estimated for $T = 110$ minutes (in Fig. 4.5). In both groups, increasing cell co-migration rates were observed for increasing threshold distances. However, for *D* values between 20 and 50 μm, values for co-migration rate were generally higher for fibroin substrates than for ProNectin substrates. For *D* values 60 μm and above, however, there was very little difference in the calculated co-migration rates for the two substrates. The increases in co-migration rate for fibroin substrates for values of *D* less than 60 μm were observed irrespective of *T* value (data not shown). Similarly, irrespective of duration time, no

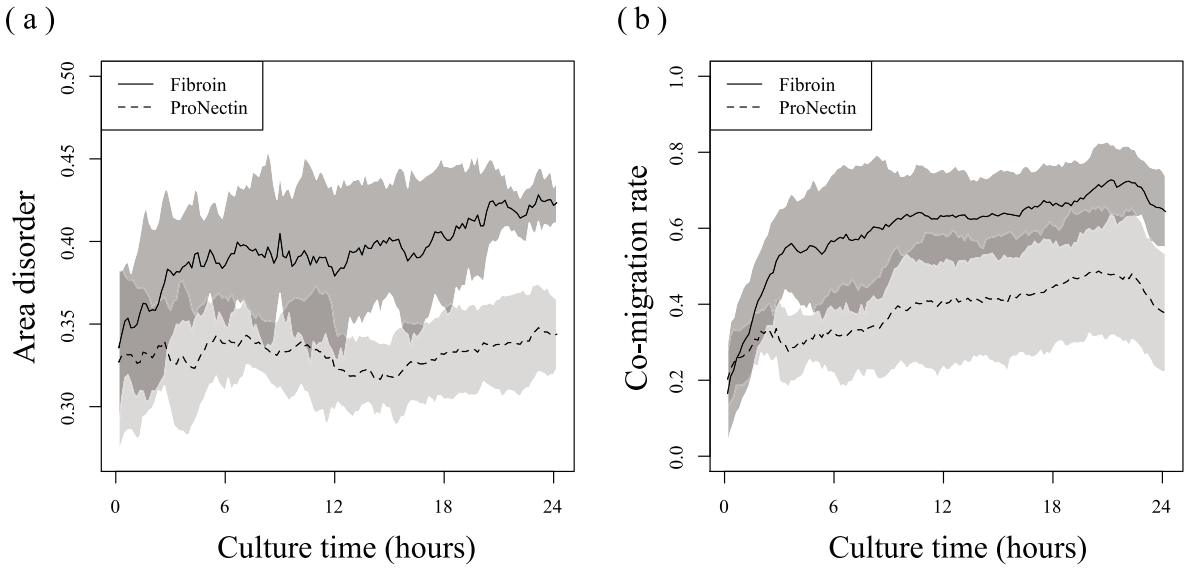

Fig. 4.3 Time dependent changes of area disorder values (a) and co-migration rate (b) in each group. The gray area indicates the standard deviation. The co-migration rates were estimated under the conditions that the threshold distance and time were 30 μm and 1 h, respectively. (n = 5)

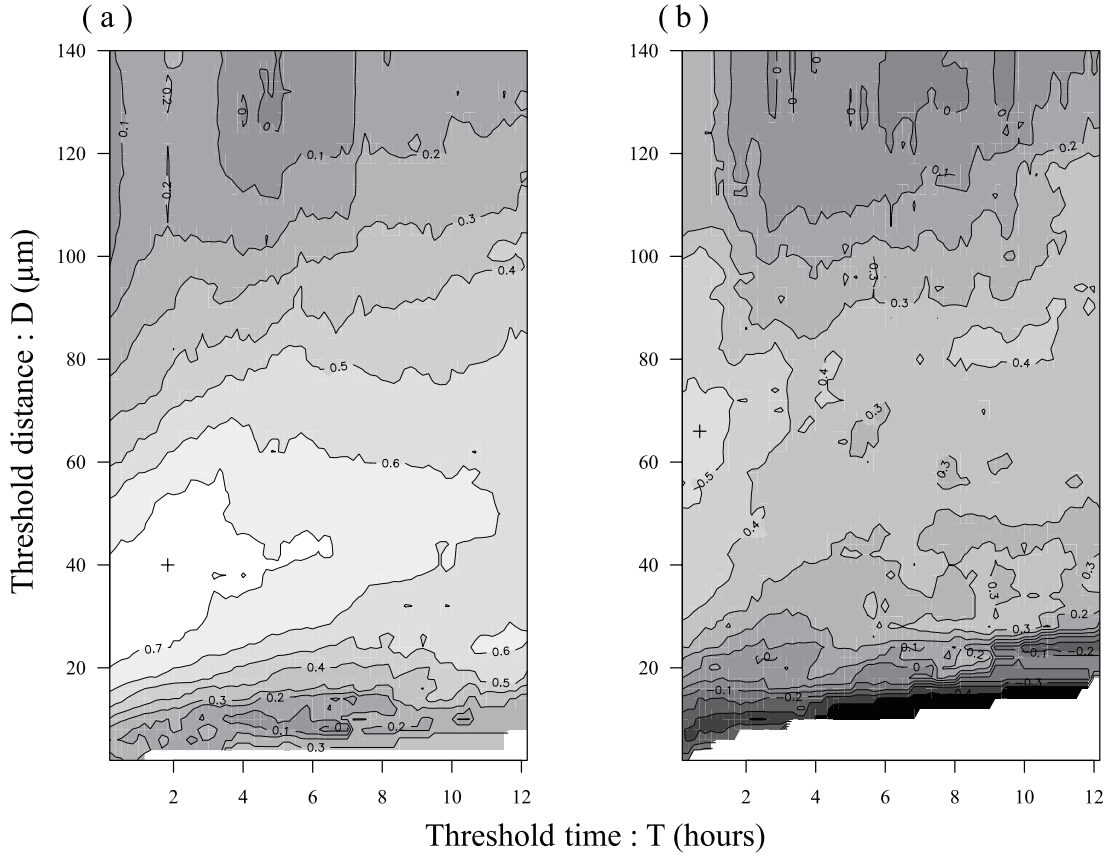

Fig. 4.4 Correlation coefficients between area distribution and co-migration rate data were plotted for the fibroin (a) and ProNectin groups (b). The threshold distance and time were sequentially increased and the co-migration rates were estimated in a round-robin fashion. The horizontal and vertical axes indicate the values of D and T, respectively. Crosses (+) indicate the maximum correlation coefficient observed in this study.

difference in co-migration rate was observed between the fibroin and ProNectin substrates for *D* values greater than 60 μm. This seems to suggest that cells exhibited different interaction behavior on fibroin and ProNectin substrates at intercellular distances of *D* = 10–60 μm. Thus, this range of *D* was adopted to estimate the probability of cell co-migration on fibroin and ProNectin substrates.

The duration time of co-migration (the time during which two cells remain within *D* μm of each other) was evaluated to investigate the stability of cell co-migration on fibroin and ProNectin substrates. Fig. 4.6 shows the estimated survival functions for cell co-migration in each group. Sample sizes for this analysis are described in Table 1. For example, under the condition of *D* = 30 μm (Fig. 4.6*c*, *solid line*), 14.3% of cell pairs remained close to each other for 6 h on fibroin substrates (95% confidence interval: 13.0–15.7%). In contrast, on ProNectin substrates, only 5.8% of cell pairs engaged in co-migration for 6 h (95% confidence interval: 4.4–7.7%), and no cell co-migration was maintained for more than 15 h (Fig. 4.6*c*, *dotted line*). Interestingly, it was found that under the condition of *D* = 60 μm, co-migration duration times were longer for the ProNectin substrates than for the fibroin substrates (Fig. 4.6*f*). In Fig. 4.7, the probability values of co-migration occurring for 110 minutes were plotted as a function of *D*. On the ProNectin substrates, the survival of cell pairs exhibiting co-migration behavior increased with *D* value (*dotted line*). For the fibroin group, the estimated probabilities of cell co-migration increased with increasing *D* value up until *D* = 30 μm. However for *D* values greater than 30 μm (*solid line*) no increase in co-migration probability was observed. This tendency was also observed independently for *T* value (data not shown). Comparing estimated probabilities of cell co-migration for fibroin and ProNectin for values of $D \leq 30$ μm, a significantly higher proportion of cell co-migrations survived on fibroin than on ProNectin substrates. Assuming that two cells are located close to each other (intercellular distance: 30 μm), the diameters of these cells would be shorter than this intercellular distance. Taking this assumption into consideration, more co-migrations of small rounded cells survived on fibroin than on ProNectin substrates under the present experimental conditions.

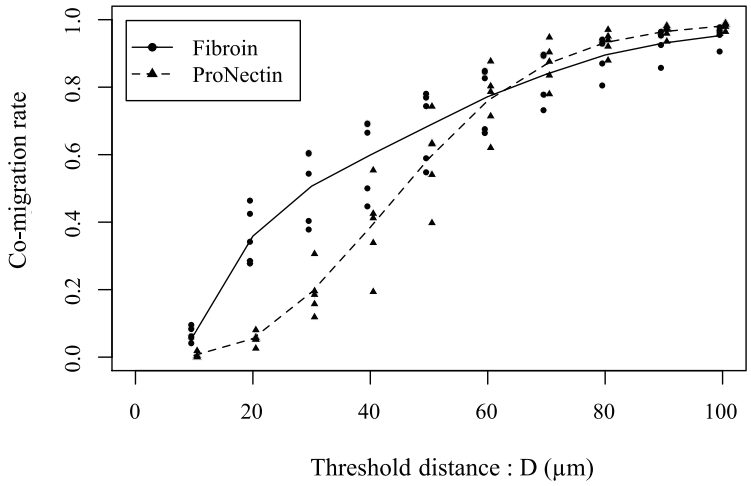

Fig. 4.5 The co-migration rate for the condition of T = 110 minutes. Horizontal axis indicates the threshold distance D. The solid line represents the mean co-migration rate for the fibroin group for different conditions of D, and the dotted line is for the ProNectin group, respectively. The co-migration rate for the fibroin group increased when $D \leq 30$ μm. For the ProNectin group, cell co-migration rate did not increase when $D \leq 20$ μm. This tendency was independent of T.

Table. 4.1 Sample size of the Kaplan-Meier survival estimates in Fig. 4.6 and Fig. 4.7.

Threshold distance: *D*	Fibroin (48–173 cells per frame)			ProNectin (64–173 cells per frame)		
	Number of events	Number of censored data	Maximum duration time [hours]	Number of events	Number of censored data	Maximum duration time [hours]
10 μm	2,543	(111)	17.8	132	(1)	6.8
20 μm	3,018	(363)	23.5	493	(7)	23.8
30 μm	2,847	(574)	24.0	997	(108)	23.8
40 μm	3,292	(751)	24.0	1,636	(246)	24.0
50 μm	4,275	(877)	24.0	2,203	(411)	24.0
60 μm	5,291	(1,061)	24.0	2,566	(598)	24.0

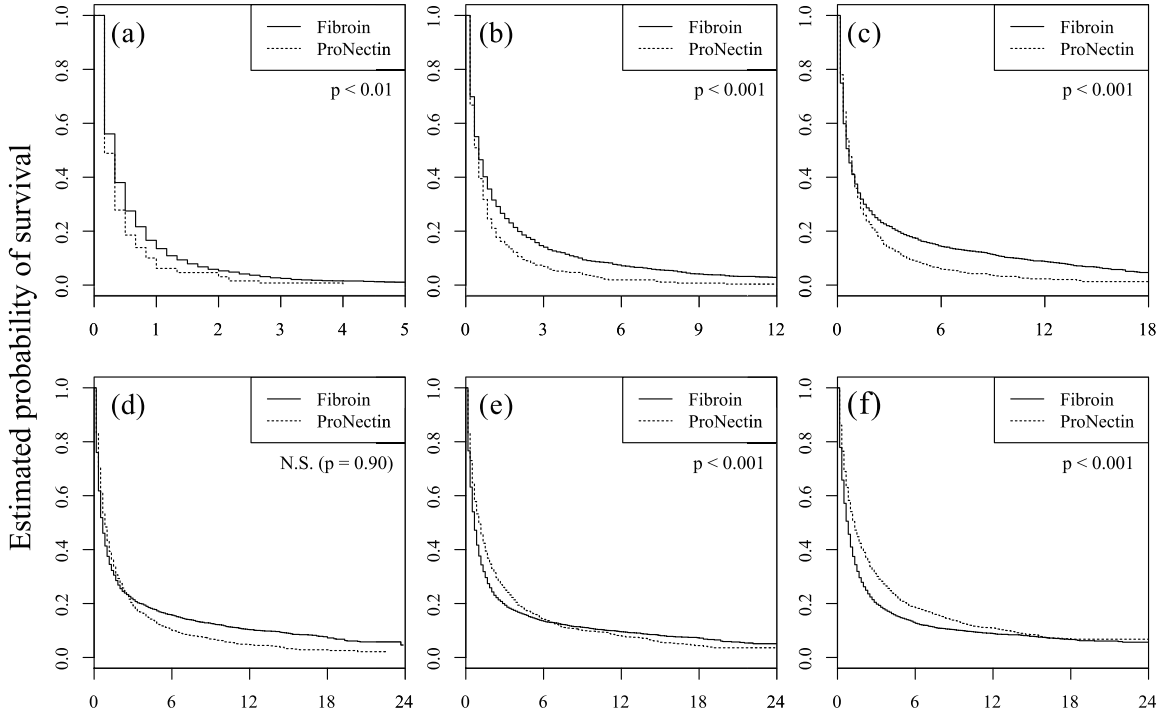

Fig. 4.6 Kaplan-Meier survival curves of cell co-migration among all cell co-migration occurrences on fibroin substrates (solid lines) and on ProNectin substrates (dotted lines). The vertical axes represent the proportion of cell co-migrations that survived the duration time, represented by horizontal axes. The plot range of duration time varied from 5 to 24 hours in order to avoid crowded figures. These survival functions were estimated for the following conditions: (a) D = 10 μm; (b) D = 20 μm; (c) D = 30 μm; (d) D = 40 μm; (e) D = 50 μm; and (f) D = 60 μm. P-value was obtained using the log-rank test. Sample sizes for this analysis are described in Table. 4.1.

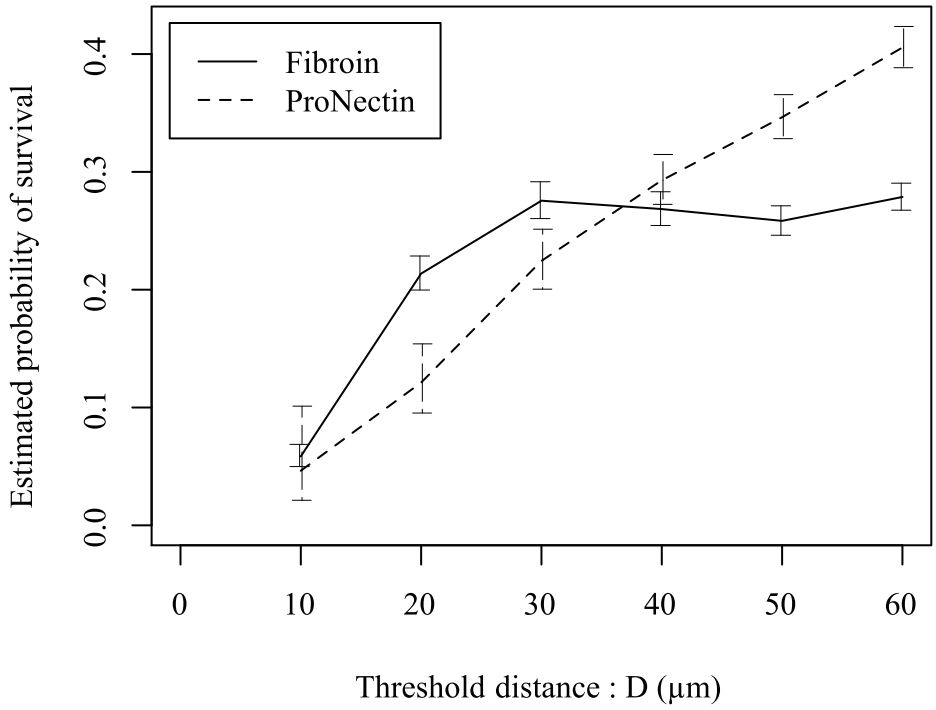

Fig. 4.7 The probability that cell co-migration survived for 110 minutes among all cell co-migration occurrences on fibroin (solid line) and ProNectin substrates (dotted line). Horizontal axis indicates the threshold distance D. The error bars indicate 95% confidence intervals. On ProNectin, the survival of cell pairs exhibiting co- migration behavior increased with D value. However, on fibroin, the estimated probabilities of cell co- migration increased steeply with $D \leq 30$ μm, but did not change for $D \geq 30$ μm. This tendency was independent of T.

4.4. DISCUSSION

Various types of experimental techniques (e.g. microscopic observations, imaging techniques, protein or gene analyses, etc.) have been carried out in the fields of tissue engineering. However, less attention has been given to cell behavior characterization techniques, despite the fact that cell-tracking techniques have been studied extensively. One promising technique is Voronoi diagram analysis, which many researchers have used for identifying spatio-temporal behavior of cell populations (8,19–22). However, the Voronoi diagram technique was insufficient for evaluating the specific behavior of individual cells. In this study, by using co-migration analysis, the different cell behavior was evaluated at a cellular level between on fibroin and ProNectin substrates.

Cell aggregation behavior is widely considered to be a primary event in this tissue formation process. In this study, a quantitative analytical approach was introduced to describe

cell co-migration. The major cell diameter for the various chondrocyte populations was found to be greater than 10 μm and less than 130 μm for both the fibroin and ProNectin groups (Fig. 4.2). From these results, a range of threshold D values of 2-180 μm, which sufficiently included suspicious cell-cell distances, were used in evaluating co-migration rate for chondrocytes on both substrates. Further Voronoi diagram analysis revealed that threshold distances larger than 60 μm were inappropriate for cell aggregation evaluation on fibroin substrates (Fig. 4.4). Fig. 4.5 also demonstrated that the difference in co-migration rates for fibroin and ProNectin substrates were most clearly seen for threshold distance D values between 10 and 60 μm. From these results, the cell co-migration rate and the duration of cell co-migration were analyzed for D = 10–60 μm.

4.4.1. Quantitative results of cell co-migration on fibroin and ProNectin substrates using a grouping method

The estimated co-migration rates revealed different distance-dependent cell behavior for the fibroin and ProNectin groups for D = 10–60 μm, while almost no differences in co-migration rate were observed for $D \geq 70$ μm (Fig. 4.5). One possible reason for this is that a threshold distance of more than 60 μm is too large to measure cell co-migration occurrences for the present cell seeding density. Interestingly, the estimated co-migration rate was measured to be about 60% for every (D, T) threshold set, which showed a strong positive correlation (more than 0.7, Fig. 4.4) with the Voronoi diagram analysis. Thus, about 60% of chondrocytes on the fibroin substrates were thought to form aggregates in this study.

The survival functions for cell co-migration also showed different distance-dependent behavior between the fibroin and ProNectin groups (Fig. 4.6 and Fig. 4.7). In the present study, the diffusion coefficient for chondrocyte migration was higher for the fibroin group than for the ProNectin group (data not shown). Hashimoto et al. also reported that a fibroin surface was able to enhance NIH 3T3 cell migration (23). Assuming that rapid migration leads to quick detachment of cells, the duration time of cell co-migration should be shorter on fibroin than on ProNectin. Looking at the duration time results, cell co-migration on fibroin was less stable than on ProNectin substrates for $D \geq 40$ μm, which was in accordance with this assumption. Interestingly, however, using a threshold distance of $D \leq 30$ μm lead to the opposite result, with the duration of cell co-migration appearing to be more stable on fibroin than on ProNectin (Fig. 4.7). Reinhart-King et al. have shown that cells can detect and respond to substrate strains created by the traction of a neighboring cell over a distance of about 30 mm (13). The present results confirmed that different cell-cell interactions were

observed within a certain intercellular distance (tens of microns) for fibroin and ProNectin groups and the different mechanical traction of substrates may lead to different cell-cell interactions on these two substrates. Additionally, Carlos et al. have shown that fibronectin fibrils polymerized into the extracellular matrix influences the shape of cell-assembly on collagen substrates (12). In order to investigate the effect of substrates on cell co-migration occurrences, it is necessary to inspect these mechanical or biochemical factors in further studies.

The survival functions for cell co-migration on fibroin substrates changed only when *D* was less than 30 μm, which may suggest that intercellular interaction is different when adjacent cells are inside or outside of 30 μm and that 30 μm may be a "critical distance" for regulating cell-cell communication on fibroin substrates. In other investigations, hyperbolic models have been used to investigate self-organized biological aggregations, and it has been shown that a model that contains spatial range for three social interactions (i.e. attractive, alignment, and repulsive) can regulate aggregation behavior (24). Additionally, Bonnet et al. investigated the cluster formation of epithelial tissue by using global attractive potential, in which cells attract one another in cell aggregate formation (25). Therefore, it may be desirable to investigate cell-cell attractive interactions with respect to cell-cell distance for distance-dependent aggregation of cells on fibroin.

4.4.2. The difference between aggregation behavior of cells on fibroin and ProNectin substrates

In a previous study, Kambe et al. measured the changes in actin polymerization, focal adhesion formation and adhesive force generation of chondrocytes on fibroin and ProNectin, and showed that the substrates had a different influence on cell morphology and adhesiveness (26). In the present study, chondrocytes expanded significantly more on ProNectin than on fibroin, which indicated that fibroin substrates might have lower cell-substrate adhesiveness than ProNectin. Reinhart-King et al. investigated cell-substrate and cell-cell adhesiveness for various densities of the RGD-ligand, and found that cell-cell contact became weak on substrates conjugated at higher densities of the ligand (13,27). Moreover, Ryan et al. reported that decreasing substratum adhesiveness might slow cell aggregation spreading over the substrate (28). These results suggest that low cell-substratum adhesiveness on fibroin probably led to the stable cell co-migration seen on fibroin substrates in this study.

4.4.3. Improvement desired for further study

There are several improvements desired for further study. It is necessary to investigate the validity of using the Kaplan-Meier estimator in further studies. Specifically, the assumption for the Kaplan-Meier plot was not sufficiently supported due to the fact that cell co-migration events were selected from combinations of cell pairs. This sampling procedure could bias the estimation of co-migration survival. It is also necessary to investigate the effect of cell shape, because the diameter of cells can have an influence on threshold distance. Moreover, the results in the present study were only useful to evaluate the cell aggregation on fibroin substrates. Therefore, more improvement is necessary before the method will be applied to other cells or substrates.

A quantitative technique for measuring cell migration is still necessary, because cell behavior is too “noisy” to distinguish qualitatively. The specific threshold distance proposed in this paper provides information for cell aggregation behavior, and the measurement of duration time for cell co-migration has made it possible to investigate cell-cell interaction quantitatively. In this respect, the grouping approach introduced in this study provides an easy and systematic way to evaluate the spatio-temporal behavior of cells on regenerative materials, and may be one promising method for tissue engineering design.

4.5. CONCLUSION

A quantitative method for measuring cell aggregation behavior was introduced to examine the mechanisms by which fibroin matrices influence cell behavior. Using the proposed method, the Kaplan-Meier results indicated that co-migration instances of rounded cells (less than 30 μm in diameter) were significantly more stable on fibroin than on ProNectin substrates under the present experimental conditions. It was also suggested that approximately 60% of chondrocytes on fibroin substrates formed cell aggregates under the present experimental conditions. The grouping approach, introduced in this study, provides an easy and systematic way to evaluate the spatio-temporal behavior of cells on regenerative materials.

4.6. APPENDIX A: GROUPING OF MOVING OBJECTS

Based on cell-cell proximity, the degree of cell aggregation was analyzed using the Grouping Method for Moving Objects, a quantitative evaluation method for analyzing the collective behavior of moving objects. Fig. 4.8 displays the conceptual diagram of this method. In this analysis, two thresholds: a threshold time (T) and distance (D) were used. Each cell was considered a moving node and these nodes were grouped using the following process.

I. The distance of each node was calculated from acquired trajectory data as a function of time.
II. From the distance dataset, every long co-migration occurrence in which two nodes located within D μm remained for more than a certain time T was recorded.
III. The rate of aggregated nodes, which exhibited long co-migration occurrences, was evaluated for each time step.

To estimate cell aggregation behavior, the rate of cells demonstrating stable co-migration was calculated as cell co-migration rate. This co-migration rate value would increase if more cells aggregated and more cell-cell contacts were formed.

Fig. 4.9 shows the process of cell co-migration analysis. From cell images (*a*), every position of the cell was tracked (*b*), and the distance between every cell pair was calculated (*c*). Fig. 4.9*d* shows an example of intercellular transition and the shaded areas represent the collision of cell i with cell j. If the duration time t of the collision was larger than the threshold time T, the cells i and j were defined as co-migrating cells and co-migration rate was evaluated. In the estimation of duration time, quantitative accuracy can be reduced by several experimental factors. Due to cell proliferation, two cells can adhere to each other soon after cell division. However, this cell colocalization was influenced not only by cell aggregation but also by the cell proliferation process. In addition, the limit in time frame or microscopic field may also reduce the accuracy. Therefore, in the Kaplan–Meier estimation, cells soon after undergoing cell division or going into frame were excluded, and out of frame cell data was referred to as censored data.

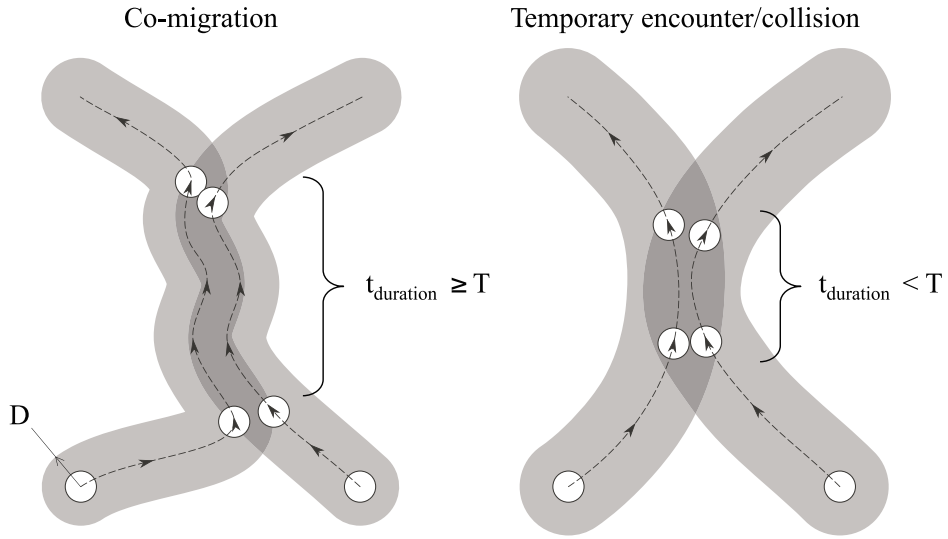

Fig. 4.8 Schematic drawing of the definition of cell co-migration. White circles indicate cells, and broken lines indicate cell trajectory. The adjacent cells, which are located less than a certain distance (D) apart, were defined as cell co-migration and the length of time over which the co-migration occurred was recorded. The co-migration maintained over the threshold time (T) was defined as stable co-migration.

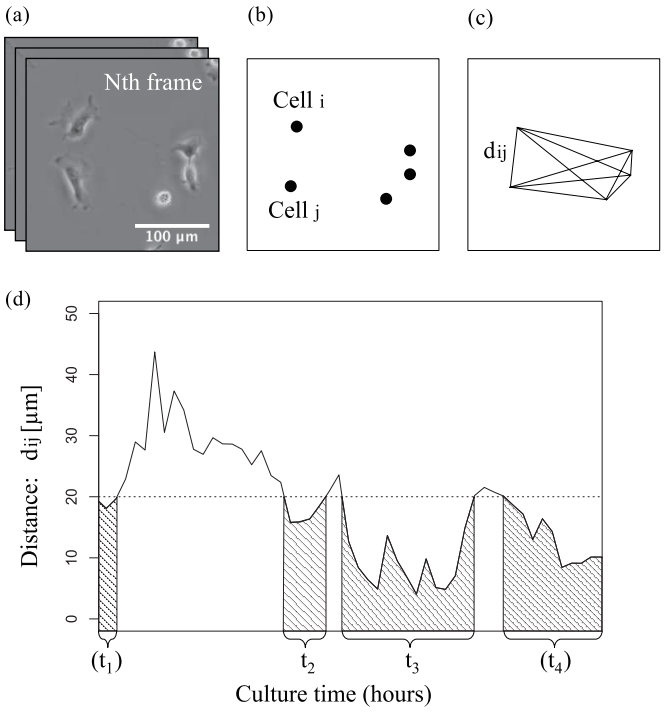

Fig. 4.9 (a-c) Process of the cell co-migration measurement.
(d) An example of intercellular distance measured in this study. While the duration time t_2 and t_3 were measured neatly, the duration time t_4 was categorized as censored data because the fourth co-migration did not reach the endpoint during time-lapse microscopy. The data for the first co-migration t1 was excluded in this analysis because the moment when the cells collided was not seen. Frame entrance or mitotic divisions of cells were excluded for the same reason.

4.7. APPENDIX B: CO-MIGRATION RATE FOR VARIOUS VALUES OF D AND T

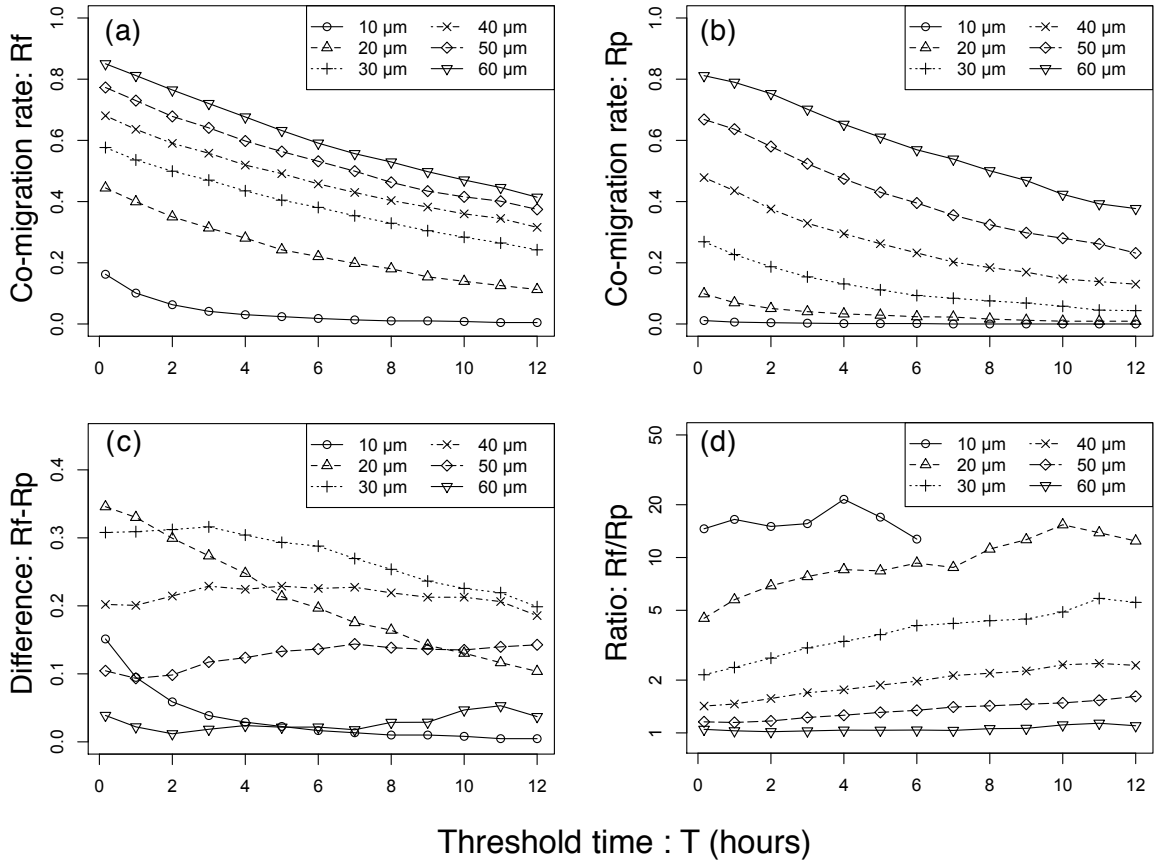

Fig. 4.10 The average plot of co-migration rate for various values of D and T. Horizontal lines indicate T, and each line represents the mean co-migration rate for different conditions of D. (a) The co-migration rate for the fibroin group (Rf) was increased when $D \leq 30$ μm. (b) For the ProNectin group, cell co-migration rate (Rp) did not increase when $D \leq 20$ μm. (c) The biphasic changes to the difference between Rf and Rp value. (d) The ratio of Rf to Rp.

4.8. REFERENCES

1. Palsson, B.O., and S.N. Bhatia. 2003. Tissue Engineering. Prentice Hall.

2. Tamada, Y. 2005. New process to form a silk fibroin porous 3-D structure. Biomacromolecules. 6: 3100–3106.

3. Fuchs, S., X. Jiang, H. Schmidt, E. Dohle, S. Ghanaati, et al. 2009. Dynamic processes involved in the pre-vascularization of silk fibroin constructs for bone regeneration using outgrowth endothelial cells. Biomaterials. 30: 1329–1338.

4. Li, C., C. Vepari, H.-J. Jin, H.J. Kim, and D.L. Kaplan. 2006. Electrospun silk-BMP-2 scaffolds for bone tissue engineering. Biomaterials. 27: 3115–3124.

5. Aoki, H., N. Tomita, Y. Morita, K. Hattori, Y. Harada, et al. 2003. Culture of chondrocytes in fibroin-hydrogel sponge. Biomed. Mater. Eng. 13: 309–316.

6. Shangkai, C., T. Naohide, Y. Koji, H. Yasuji, N. Masaaki, et al. 2007. Transplantation of allogeneic chondrocytes cultured in fibroin sponge and stirring chamber to promote cartilage regeneration. Tissue Eng. 13: 483–492.

7. Kawakami, M., N. Tomita, Y. Shimada, K. Yamamoto, Y. Tamada, et al. 2011. Chondrocyte distribution and cartilage regeneration in silk fibroin sponge. Biomed. Mater. Eng. 21: 53–61.

8. Otaka, A., N.D. Kachi, N. Hatano, Y. Kuwana, Y. Tamada, et al. 2013. Observation and quantification of chondrocyte aggregation behavior on fibroin surfaces using voronoi partition. Tissue Eng. Part C. Methods. 19: 396–404.

9. Suzuki, K.G.N., T.K. Fujiwara, F. Sanematsu, R. Iino, M. Edidin, et al. 2007. GPI-anchored receptor clusters transiently recruit Lyn and G alpha for temporary cluster immobilization and Lyn activation: single-molecule tracking study 1. J. Cell Biol. 177: 717–730.

10. Suzuki, K.G.N., T.K. Fujiwara, M. Edidin, and A. Kusumi. 2007. Dynamic recruitment of phospholipase C gamma at transiently immobilized GPI-anchored

receptor clusters induces IP3-Ca2+ signaling: single-molecule tracking study 2. J. Cell Biol. 177: 731–742.

11. Kim, M.-H., M. Kino-oka, Y. Morinaga, Y. Sawada, M. Kawase, et al. 2009. Morphological regulation and aggregate formation of rabbit chondrocytes on dendrimer-immobilized surfaces with D-glucose display. J. Biosci. Bioeng. 107: 196–205.

12. Szabó, B., G. Szöllösi, B. Gönci, Z. Jurányi, D. Selmeczi, et al. 2006. Phase transition in the collective migration of tissue cells: Experiment and model. Phys. Rev. E. 74: 061908.

13. Kachi, N.D., A. Otaka, S. Sim, Y. Kuwana, Y. Tamada, et al. 2010. Observation of chondrocyte aggregate formation and internal structure on micropatterned fibroin-coated surface. Biomed. Mater. Eng. 20: 55–63.

14. Reinhart-King, C. a, M. Dembo, and D. a Hammer. 2008. Cell-cell mechanical communication through compliant substrates. Biophys. J. 95: 6044–6051.

15. Vicsek, T., and A. Zafeiris. 2012. Collective motion. Phys. Rep. 517: 71–140.

16. Cappello, J., and J.W. Crissman. 1990. The Design and Production of Bioactive Protein Polymers For Biomedical Applications. Polym. Prepr. 31: 193–194.

17. Anderson, J.P., J. Cappello, and D.C. Martin. 1994. Morphology and primary crystal structure of a silk-like protein polymer synthesized by genetically engineered Escherichia coli bacteria. Biopolymers. 34: 1049–1058.

18. Meijering, E., O. Dzyubachyk, and I. Smal. 2012. Methods for cell and particle tracking. In: Methods in enzymology. Elsevier Inc. pp. 183–200.

19. Marcelpoil, R., and Y. Usson. 1992. Methods for the study of cellular sociology: Voronoi diagrams and parametrization of the spatial relationships. J. Theor. Biol. 154: 359–369.

20. Eftimie, R. 2012. Hyperbolic and kinetic models for self-organized biological aggregations and movement: a brief review. J. Math. Biol. 65: 35–75.

21. Bonnet, N., M. Matos, M. Polette, J.-M. Zahm, B. Nawrocki-Raby, et al. 2004. A density-based cellular automaton model for studying the clustering of noninvasive cells. IEEE Trans. Biomed. Eng. 51: 1274–1276.

22. Kambe, Y., K. Yamamoto, K. Kojima, Y. Tamada, and N. Tomita. 2010. Effects of RGDS sequence genetically interfused in the silk fibroin light chain protein on chondrocyte adhesion and cartilage synthesis. Biomaterials. 31: 7503–7511.

23. Reinhart-King, C. a, M. Dembo, and D. a Hammer. 2005. The dynamics and mechanics of endothelial cell spreading. Biophys. J. 89: 676–689.

24. Ryan, P.L., R.A. Foty, J. Kohn, and M.S. Steinberg. 2001. Tissue spreading on implantable substrates is a competitive outcome of cell-cell vs. cell-substratum adhesivity. Proc. Natl. Acad. Sci. U. S. A. 98: 4323–4327.

25. Palecek, S.P., J.C. Loftus, M.H. Ginsberg, D.A. Lauffenburger, and A.F. Horwitz. 1997. Integrin-ligand binding properties govern cell migration speed through cell-substratum adhesiveness. Nature. 385: 537–540.

26. Hashimoto, T., K. Kojima, A. Otaka, Y.S. Takeda, N. Tomita, et al. 2013. Quantitative evaluation of fibroblast migration on a silk fibroin surface and TGFBI gene expression. J. Biomater. Sci. Polym. Ed. 24: 158–169.

Chapter 5.
How do chondrocytes aggregate on fibroin substrate

5.1. INTRODUCTION

Cell migration within a three-dimensional matrix and over two-dimensional substrates occurs in a wide variety of physiological and biotechnological situations, such as tissue repair, immune response reactions, and tumor invasion (1). Various stimuli from the surrounding environment are known to affect cell behavior; for example, changes in cell-cell adhesion may initiate cell migration. On the other hand, cell-substrate adhesion also has an important role in regulating cell migration behavior. Hence the effects of substrate mechanics on cell behavior have been under intense investigation.

Fibroin, which is one of the component proteins in silk, and has been widely used in biomedical applications (2–4). Moreover, in the field of cartilage regeneration, many researchers have investigated its application as a cell scaffold (5, 6). Kawakami et al. used a fibroin sponge as a scaffold for chondrocyte cultivation and demonstrated that initial chondrocyte aggregation led to an enhanced cartilage tissue formation in fibroin sponges (7). In addition, in chapter 2, we investigated cell aggregation behavior on fibroin substrates, and noted that fibroin was able to enhance cell-cell interactions during cultivation and control cell aggregation behavior during cell migration (8). In general, cell aggregation is one of the key events in cell-cell interaction, making it a vital part of tissue formation. From both scientific and engineering viewpoints, the understanding of the cell-cell adhesion process is important for clarifying and regulating cell aggregation and subsequent tissue formation for various biomaterial (e.g. fibroin).

In this chapter, cell proximity behavior on fibroin substrates was quantitatively evaluated focusing on two aspects: the distance and the direction of multi-cell movement. Cell-cell distance and its dynamic changes are one of the key factors for characterizing the cell-cell adhesion process. Reinhart-King et al. researched the contribution of matrix mechanics to stable cell-cell contact and suggested that matrix stiffness determined the length over which cells can detect adjacent cells (9). By understanding the distance in which cell detect surrounding cells, it is possible to gain insights into the cell aggregation mechanism on fibroin. Moreover, cell migration is a multi dimension behavior and its directionality may be another factor in determining cell-cell interaction. In this chapter, the distance between cells

and the direction of cell migrations cultured on fibroin substrates were measured in order to evaluate cell aggregation behavior on fibroin substrates.

5.2. MATERIALS AND METHODS

5.2.1. Cell preparation

Articular cartilage tissue was aseptically removed from the proximal humerus, distal femur, and proximal tibia of 4-week-old Japanese White rabbits (Oriental Bio Service, Kyoto, Japan). After all adherent connective tissue had been removed, the excised cartilage tissue was diced into 1 mm^3 segments and chondrocytes were isolated by digesting small segments of cartilage with 0.25% trypsin EDTA (Nacalai Tesque, Kyoto, Japan) for 30 minutes in a temperature controlled bath at 37°C. After being rinsed twice with Dulbecco's Phosphate Buffered Saline (PBS; Nacalai Tesque, Kyoto, Japan) and centrifuged at 1500 rpm for 5 minutes, the cartilage was enzymatically digested with 0.25% type II collagenase (CLS-2; Worthington Biochemical, Lakewood, NJ) for 6 hours at 37°C. After straining through a cell strainer (BD Falcon, Franklin Lakes, NJ) and washing twice with PBS, a single cell suspension was obtained. Cartilage harvests from living animals were approved and accepted by the animal care committee of the Institute for Frontier Medical Sciences at Kyoto University.

Cells were passaged once with Dulbecco's modified Eagle's medium (DMEM; Nacalai Tesque, Kyoto, Japan) containing 10% fetal bovine serum (FBS; Nacalai Tesque, Kyoto, Japan) and 1% antibiotic mixture (10,000 units/mL penicillin, 10,000 mg/mL streptomycin, and 25 mg/mL amphotericin B; Nacalai Tesque, Kyoto, Japan) beforehand. Cells were cultured at 37°C in a humidified atmosphere of 95% air and 5% CO2 for 5 days. The medium was changed every 2 days.

5.2.2. Substrates plates preparation

To create fibroin coated plates, an aqueous fibroin solution was prepared as described previously. Briefly, degummed silk fibroin fibers of Bombyx mori cocoons were dissolved in 9 M lithium bromide aqueous solution at room temperature, and then the solution was dialyzed against pure water. The concentration of fibroin in the water solution was determined by colorimetric method and was prepared to be 1 wt%. Before coating the fibroin substrate, 35 mm glass bottom dishes (27 mm glass coverslip in diameter; Asahi Techno Grass, Tokyo, Japan) were washed with acetone and completely dried at 50°C. Culture dishes

were soaked in fibroin solution for 1 min at room temperature, and then dried at 50°C. The dishes were immersed in 80% methanol solution for 1 hour, and dried again at 50°C.

To create protein coated cell adhesive plates, ProNectin F (Sanyo Chemical Industries, Kyoto, Japan), which was composed of RGD amino sequences and silk fibroin beta-sheet structures, was prepared according to the manufacturer's instructions. Briefly, stock solution was diluted to 10 μg/mL in PBS at 37°C. Culture dishes were soaked in the diluted solution for 5 min at room temperature. Afterward, the culture dishes were washed twice with PBS.

5.2.3. Time-lapse microscopy and cell trajectory acquisition

Passaged chondrocytes were removed from the T flasks by adding 0.25% trypsin EDTA and washed twice with PBS. Soon after, detached cells were suspended in Leibovitz's L-15 medium (Invitrogen, Carlsbad, CA) containing 10 vol% FBS, 1 vol% antibiotic mixture and 0.2 mM ascorbic acid (A8960; Sigma-Aldrich Japan, Tokyo, Japan). After that, 1.0×10^5 cells were seeded on a dish in cell suspension medium at a concentration of 5.0×10^4 cells/mL (at a density of approximately 1×10^4 cells/cm^2).

Each dish was enclosed in a culture chamber (MI-IBC-IF; Olympus, Tokyo, Japan) in a humidified atmosphere at 37°C and placed on an inverted phase microscope (IX-81; Olympus, Tokyo, Japan). During a 24-hour culture, time-lapse phase contrast images were captured every 10 minutes by a CCD camera (DP70; Olympus, Tokyo, Japan). The image size was 680 × 512 pixels at 1.3 μm resolution.

Every cell captured in time-lapse observation on each substrate (fibroin and ProNectin; n = 5 each) was manually tracked using MTrackJ (10), an ImageJ (National Institutes of Health, Bethesda, MD) tracking plugin. Position data of each cell on each frame was measured by the MTrackJ tracking function and was recorded in spreadsheets to calculate distances between each pair of cells and the direction of cell motion.

5.2.4. Two cell proximity evaluation

From trajectory data, the Euclidean distance between each pair of cells was measured and the period for which cells remained within a certain distance L was recorded using R (The R Foundation for Statistical Computing, Vienna, Austria). In practice, some cells move into/out of frame during time-lapse observation. Therefore, the Kaplan–Meier estimator was used and out of frame cell data was referred to as censored data. In addition, cell pairs that emerged simultaneously because of frame entrance or mitotic division were excluded in this analysis.

5.2.5. Direction of cell migration

In order to assess whether the direction of cell migration enhanced aggregation behavior, a density-based evaluation, which was a modified cell migration analysis method based on Bonnet et al. (11), was used. Specifically, cell density distributions were evaluated using two-dimensional Kernel density estimation, and subsequently the gradient of the density field was computed. Cell migration direction was measured from cell trajectory data and the relationships between cell migration and density gradient directions were evaluated. In this study, index was used to characterize the difference in cell migration direction on each substrate, and an increase/decrease in index meant that there were attractive/repulsive movements in the cells' spatio-temporal behavior, respectively (see Appendix A).

5.2.6. Cell size measurement

The diameters of round shaped cell were evaluated by using ImageJ. Cells on fibroin substrates were chosen at random and each cell's diameter was measured manually. Assuming that two cells were in direct contact with each other, the distance between them would be the average of their diameters.

5.2.7. Statistical tests

The Kaplan–Meier estimator was used to calculate the survival function for cell proximity data for the fibroin and ProNectin groups, and a statistical comparison of survival function was done using the log-rank test. Chi-square tests were used to evaluate heterogeneity of the angle between cell migrations and density gradient directions. The difference between index on fibroin and ProNectin was analyzed with Welch's t-test. All tests were performed with a significance level of 0.05.

5.3. RESULTS

5.3.1. Cells maintained rounded shapes on fibroin substrates

Chondrocytes were seeded on each substrate at high density (1×10^4 cells/cm^2) and the distance between each cell and the cell migration directions were evaluated. On the ProNectin substrate, cells elongated and few cells were found to be in contact with each other (see Chapter. 4.) On the fibroin substrate, however, many chondrocytes maintained a rounded shape and participated in cell aggregation. The size of the round cells on fibroin substrates

ranged from 10 to 20 μm in diameter (see Fig. 5.1).

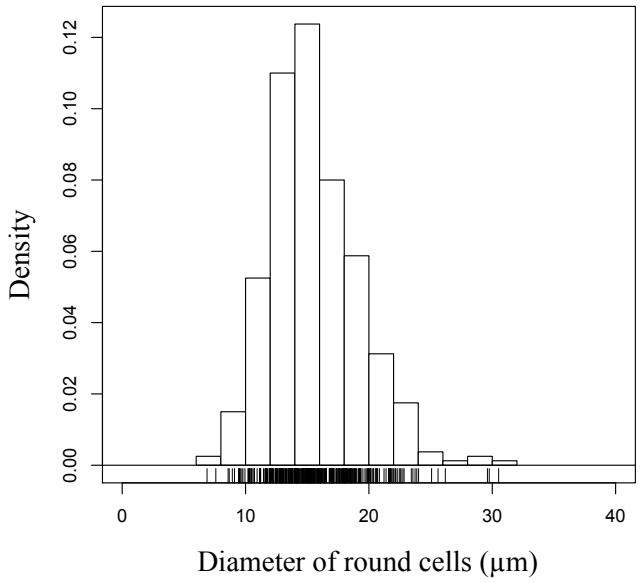

Fig. 5.1 Histogram of the diameters of rounded shape chondrocytes cultured on the fibroin surfaces. N = 401.

5.3.2. Cells on fibroin remain close to adjacent cells

In Fig. 5.2, histograms for the distance between each pair of cells on the different substrate are shown. On fibroin substrates, the number of cell pairs peaked when the two cells were located less than 20 μm apart. However, ProNectin substrates did not show this tendency. From this result, we focused on 20 μm because this distance was supposed to be a characteristic distance for cell aggregation behavior on fibroin substrates.

Fig. 5.3 shows the estimated survival functions of cell proximity-maintaining behavior, which means that cells remain within 20 μm of an adjacent cell. On fibroin substrates, 31 percent of cell pairs remained close to each other for 1 hour (95% confidence interval, 30–33 percent), while 20 and 15 percent remained close for 2 or 3 hours, respectively. On the other hand on ProNectin substrates, 21 percent of cell pairs remained close to each other for 1 hour (95% confidence interval, 18–25 percent) and no cell proximity maintained more than 15 hours.

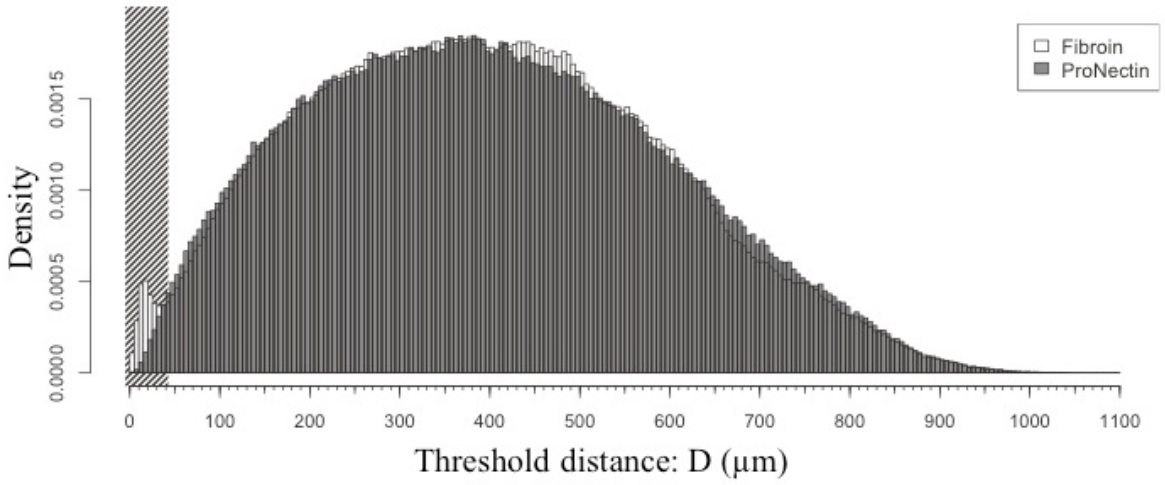

Fig. 5.2 The distribution of computed distance between each pair of cells on the fibroin substrate. A peak was found in cell-cell distance distribution on fibroin, which was not found on ProNectin (the shaded region).

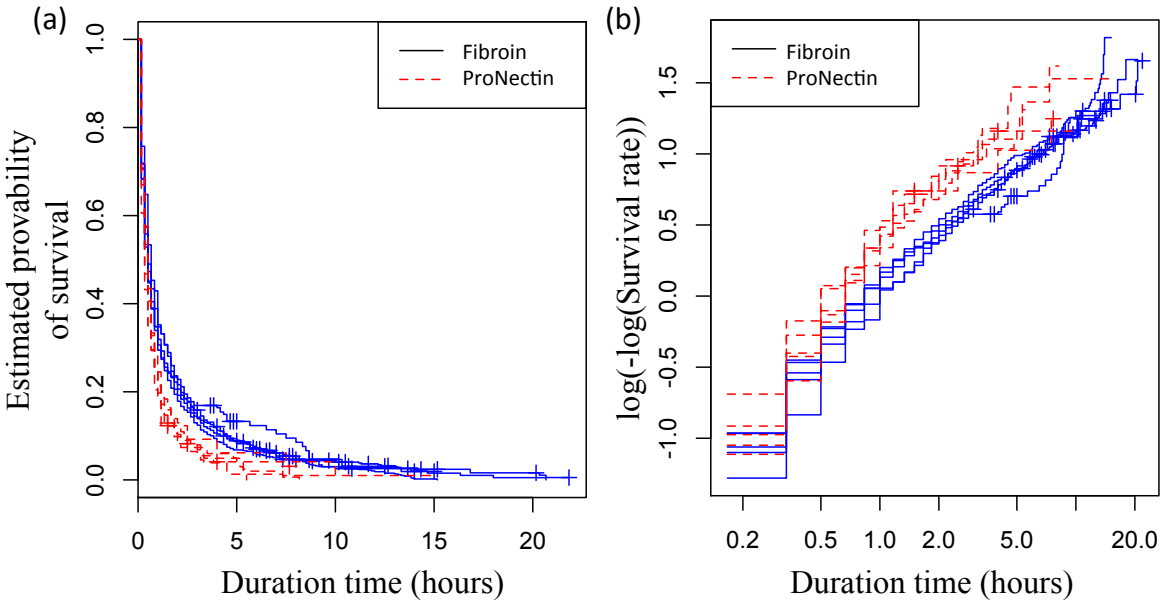

Fig. 5.3 Estimated survival functions (a) and log-log plot (b) of cell proximity-maintaining behavior. Duration time of cell proximity maintainance was significantly different between fibroin and ProNectin substrates (log-rank test; $p < 10^{-6}$). Total sample size was 3855 (including 455 censored data points) for fibroin and 777 (including 39 censored data points) for ProNectin.

5.3.3. Direction of cell migration on fibroin was not biased by cell density

Fig. 5.4 shows the distribution of angles between migration direction and cell density gradient on each substrate. Radial axes represent the ratio of actual frequency relative to an ideal frequency distributed evenly over 180 degrees. Therefore, plots with concentric circles indicate that there is no relationship between migration direction and cell density. On ProNectin substrates, 53 percent of cells moved to areas of lower cell density. On the other hand, there were no relationships between cell migration and density gradients on fibroin substrates.

Furthermore, the index for ProNectin was smaller than that for fibroin and there was a significant difference between the two groups (Welch's t-test $p < 0.005$; Chapter 4). This difference in the direction of cell migration could be a possible reason for the different cell aggregation behaviors on each substrate.

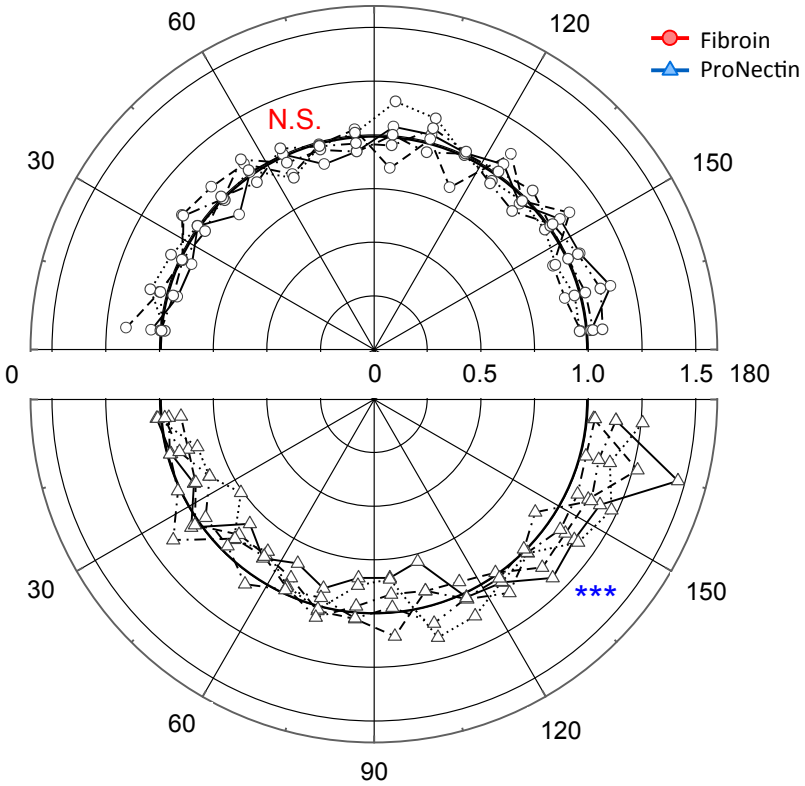

Fig. 5.4 Distribution of the angles θ. The statistical heterogenousity of the angles θ on each substrate was evaluated with Pearson's chi-squared test ($p < 0.05$). *** $p < 0.001$. Sample size was 19,995 for fibroin and 16,425 for ProNectin.

5.4. DISCUSSION

Cell migration on fibroin and ProNectin substrates was observed using phase-contrast microscopy, and the distance between cell pairs and the direction of cell migration were evaluated. The results demonstrated that cell behavior was completely different on fibroin and ProNectin substrates. Cell proximity behavior was observed more frequently and for longer on fibroin substrates compared to ProNectin. However, no attractive behavior was observed on fibroin, whereas cells on ProNectin tended to migrate into areas of lower cell density.

Substrate material and the surrounding environment provide many types of stimuli and influence cell behavior in many ways (12). For example, Petrie et al. noted that factors such as the topography of the extracellular matrix and receptor signaling promoted directional migration (13). It is widely said that balance between cell–cell and cell–substrate adhesion is one of the important factors in cell aggregate formation. Moreover, Kambe et al. measured the adhesive force of chondrocytes on fibroin and ProNectin, and discussed the possibility of the substrates' effects on chondrocyte's phenotypes (14). Taking the above into consideration, low cell-substratum adhesiveness probably led to the stable cell proximity behaviors seen on fibroin substrates in this study.

Abercrombie et al. proposed the existence of contact inhibition of locomotion (CIL), in which a migrating cell in contact with another migrating cell changes direction to move away from the point of contact (15, 16). This mechanism is still not fully understood. However, it is generally said that cell-substratum adhesiveness is one of the possible causes for cell protrusions and migrations (17). From this, cell density dependent migration observed in this study could be caused by adhesion provided on ProNectin substrates. Moreover, the fibroin surface might suppress CIL, influencing cell aggregation formation.

5.5. CONCLUSION

We performed two types of evaluation for different cell aggregation behavior. The results showed that cell proximity behavior was observed more frequently and for longer on fibroin than on ProNectin. However, no attractive behavior was observed in cell aggregation on fibroin, whereas cells on ProNectin tended to migrate into areas of lower cell density.

5.6. APPENDIX: CELL MIGRATION ANALYSIS

The relationship between the direction of cell migration and the gradient of cell density was evaluated using the following procedure.

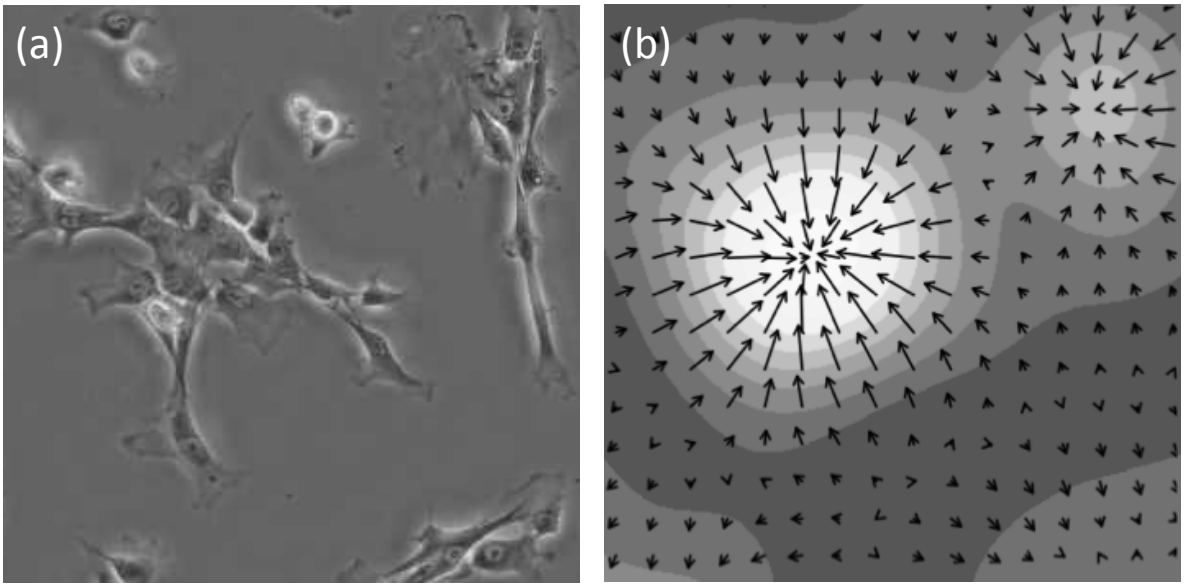

Fig. 5.5 Schematic image of estimation of cell density gradient

- The direction of cell migration $\boldsymbol{v}_i(t)$ was computed for the different images at a time of t and $t + Dt$.
- A potential field based on the local density of cells is computed according to the two-dimensional Kernel density estimation: the density of cells at position $\boldsymbol{x}$ is computed as a function of the positions of cells $\boldsymbol{x}_i$, according to

$$f(\boldsymbol{x},t) = \frac{1}{nh^2}\sum_i^n \mathrm{K}\left(\frac{\boldsymbol{x}-\boldsymbol{x}_i}{h}\right) \qquad \text{(A1)}$$

  where n is the total cell number, h is the bandwidth and K is the kernel function. Gaussian kernel was used in this study. (see Fig. 5.5b)
- The gradient of the cell density field $\boldsymbol{n}(\boldsymbol{x},\mathrm{t})$ at position $\boldsymbol{x}$ in each frame t was computed. After $\boldsymbol{v}_i(\mathrm{t})$ and $\boldsymbol{n}(\boldsymbol{x}_i,\mathrm{t})$ were calculated, the correlation of these two vectors was calculated for each cell i, as follows.

$$\cos\theta = \frac{\boldsymbol{v}\cdot\boldsymbol{n}}{|\boldsymbol{v}||\boldsymbol{n}|} \qquad \text{(A2)}$$

- In order to evaluate the tendencies of cell density-based migration, weighted average of $\cos\theta$ values over the total number of cells and frames was calculated. This *index* ranges from -1 to 1 as its value is increased or decreased by attractive or repulsive behavior in the cell population, respectively.

$$index = \frac{\sum_{i,t}(|\boldsymbol{n}(\boldsymbol{x}_{i,t},t)|\cos\theta_{i,t})}{\sum_{i,t}|\boldsymbol{n}(\boldsymbol{x}_{i,t},t)|} \qquad \text{(A3)}$$

As is customary, cells located in border zones of the image were excluded from this migration analysis, as no correct density information relating to their final distribution can be taken from the image. The bandwidth h was 51 μm in this study.

5.7. REFERENCES

1. Palsson, B.O., and S.N. Bhatia. 2003. Tissue Engineering. Prentice Hall.

2. Gotoh, K., H. Izumi, T. Kanamoto, Y. Tamada, and H. Nakashima. 2000. Sulfated fibroin, a novel sulfated peptide derived from silk, inhibits human immunodeficiency virus replication in vitro. Biosci. Biotechnol. Biochem. 64: 1664–1670.

3. Min, B.-M., G. Lee, S.H. Kim, Y.S. Nam, T.S. Lee, et al. 2004. Electrospinning of silk fibroin nanofibers and its effect on the adhesion and spreading of normal human keratinocytes and fibroblasts in vitro. Biomaterials. 25: 1289–1297.

4. Hofmann, S., C.T.W.P. Foo, F. Rossetti, M. Textor, G. Vunjak-Novakovic, et al. 2006. Silk fibroin as an organic polymer for controlled drug delivery. J. Control. Release. 111: 219–227.

5. Aoki, H., N. Tomita, Y. Morita, K. Hattori, Y. Harada, et al. 2003. Culture of chondrocytes in fibroin-hydrogel sponge. Biomed. Mater. Eng. 13: 309–316.

6. Wang, Y., D.J. Blasioli, H.-J. Kim, H.S. Kim, and D.L. Kaplan. 2006. Cartilage tissue engineering with silk scaffolds and human articular chondrocytes. Biomaterials. 27: 4434–4442.

7. Kawakami, M., N. Tomita, Y. Shimada, K. Yamamoto, Y. Tamada, et al. 2011. Chondrocyte distribution and cartilage regeneration in silk fibroin sponge. Biomed. Mater. Eng. 21: 53–61.

8. Otaka, A., N.D. Kachi, N. Hatano, Y. Kuwana, Y. Tamada, et al. 2012. Observation and quantification of chondrocyte aggregation behavior on fibroin surfaces using Voronoi Partition. Tissue Eng. Part C. Methods. : 1–2.

9. Reinhart-King, C. a, M. Dembo, and D. a Hammer. 2008. Cell-cell mechanical communication through compliant substrates. Biophys. J. 95: 6044–6051.

10. Meijering, E., O. Dzyubachyk, and I. Smal. 2012. Methods for cell and particle tracking. In: Methods in enzymology. Elsevier Inc. pp. 183–200.

11. Bonnet, N., M. Matos, M. Polette, J.-M. Zahm, B. Nawrocki-Raby, et al. 2004. A density-based cellular automaton model for studying the clustering of noninvasive cells. IEEE Trans. Biomed. Eng. 51: 1274–1276.

12. Owen, S.C., and M.S. Shoichet. 2010. Design of three-dimensional biomimetic scaffolds. J. Biomed. Mater. Res. A. 94: 1321–1331.

13. Petrie, R.J., A.D. Doyle, and K.M. Yamada. 2009. Random versus directionally persistent cell migration. Nat. Rev. Mol. Cell Biol. 10: 538–549.

14. Kambe, Y., K. Yamamoto, K. Kojima, Y. Tamada, and N. Tomita. 2010. Effects of RGDS sequence genetically interfused in the silk fibroin light chain protein on chondrocyte adhesion and cartilage synthesis. Biomaterials. 31: 7503–7511.

15. Abercrombie, M., and J.E.M. Heaysman. 1954. Observations on the social behaviour of cells in tissue culture. Exp. Cell Res. 6: 293–306.

16. Abercrombie, M., and J.E.M. Heaysman. 1953. Observations on the social behaviour of cells in tissue culture. Exp. Cell Res. 5: 111–131.

17. Palecek, S.P., J.C. Loftus, M.H. Ginsberg, D.A. Lauffenburger, and A.F. Horwitz. 1997. Integrin-ligand binding properties govern cell migration speed through cell-substratum adhesiveness. Nature. 385: 537–540.

List of publications

1. ORIGINAL PAPERS

Chapter 2.

Akihisa Otaka, Naoyoshi D Kachi, Naoya Hatano, Yoshihiko Kuwana, Yasushi Tamada, and Naohide Tomita. Observation and Quantification of Chondrocyte Aggregation Behavior on Fibroin Surfaces Using Voronoi Partition. *Tissue Engineering Part C: Methods*, (2013), 19: 396-404.

Chapter 4.

Akihisa Otaka, Kazuya Takahashi, Yuji S Takeda, Yusuke Kambe, Yoshihiko Kuwana, Yasushi Tamada, and Naohide Tomita. Quantification of Cell Co-migration Occurrences During Cell Aggregation on Fibroin Substrates. *Tissue Engineering Part C: Methods*, In printing.

2. CONFERENCE PUBLICATIONS

Chapter 5.

Akihisa Otaka, Kazuya Takahashi, Kenji Isshiki, Yusuke Kambe, Katsura Kojima, Yasushi Tamada, and Naohide Tomita. How do chondrocytes aggregate on fibroin substrate. *Conference proceedings: the 35th Annual International Conference of the IEEE Engineering in Medicine and Biology Society.* (2013), 405-408.

3. INTERNATIONAL CONFERENCES

Akihisa Otaka, Yasuhiro Shimada, Masahiro Kawakami, Naoyoshi D Kachi, Koji Yamamoto, Yasushi Tamada, and Naohide Tomita. Quantitative Evaluation of Cell Aggregating Process at Early Stage of Cartilage Regeneration. *The 56th Annual Meeting of the Orthopaedic Research Society*. (2010), New Orleans, Louisiana, USA.

Yuji S Takeda, Akihisa Otaka, Yasushi Tamada, and Naohide Tomita. Quantification of the relationship between cell shape and intercellular adhesion of chondrocytes on a fibroin substrate, *The 23rd European Conference on Biomaterials*. (2010), Tampere, Finland.

Akihisa Otaka, Kazuya Takahashi, Kenji Isshiki, Yusuke Kambe, Katsura Kojima, Yasushi Tamada, and Naohide Tomita. How do chondrocytes aggregate on fibroin substrate. *The 35th Annual International Conference of the IEEE Engineering in Medicine and Biology Society*. (2013), Osaka, Japan.

Kenji Isshiki, Akihisa Otaka, Kazuya Takahashi, Katsura Kojima, Yasushi Tamada and Naohide Tomita. Quantification of density dependent migration of cells on fibroin substrate. *The 19th Congress of the European Society of Biomechanics*. (2013), Patras, Greece.

4. DOMESTIC CONFERENCES

Akihisa Otaka, Naoyoshi D Kachi, Yoshihiko Kuwana, Yasushi Tamada and Naohide Tomita. Observation and quantification of cell aggregation behavior on fibroin substrates, *The 36th Annual Meeting of the Japanese Society for Clinical Biomechanics*. (2009), Ehime.

Akihisa Otaka, Naoyoshi D Kachi, Seungwoo Sim, Yoshihiko Kuwana, Yasushi Tamada and Naohide Tomita. Observation and quantification of chondrocyte aggregation on fibroin substrates, *The 31st Annual Meeting of the Japanese Society for Biomaterials*, (2009), Kyoto.

Naoyoshi D Kachi, Akihisa Otaka, Seungwoo Sim, Yoshihiko Kuwana, Yasushi Tamada and Naohide Tomita. Quantification of chondrocyte aggregation and matrix synthesis on micropatterned fibroin-coated surface, *The 30th Japanese Biotribology Symposium*, (2010), Fukuoka.

Akihisa Otaka, Naoyoshi D Kachi, Seungwoo Sim, Yoshihiko Kuwana, Yasushi Tamada and Naohide Tomita. Observation of chondrocyte aggregation on fibroin substrates, *The 9th Congress of the Japanese Society for Regenerative Medicine*. (2010), Hiroshima.

Yuji S Takeda, Akihisa Otaka, Katsura Kojima, Yasushi Tamada and Naohide Tomita. Chondrocyte aggregate formation on L-RGDSx2-induced fibroin substrates, *The 9th Congress of the Japanese Society for Regenerative Medicine*. (2010), Hiroshima.

Akihisa Otaka, Naoyoshi D Kachi, Yuji S Takeda, Seungwoo Sim, Yoshihiko Kuwana, Yasushi Tamada and Naohide Tomita. Cell Sociological approach for tissue engineering: Observation and quantification of chondrocyte aggregate behavior on fibroin substrates, *SICE SSI 2010*, (2010), Kyoto.

Yuji S Takeda, Akihisa Otaka, Yasushi Tamada and Naohide Tomita. Quantification of chondrocyte aggregate behavior on fibroin substrates, *The 10th Congress of the Japanese Society for Regenerative Medicine*. (2011), Tokyo.

Akihisa Otaka, Yasushi Tamada, Yoshihiko Kuwana, Naoya Hatano and Naohide Tomita. Quantification of the effect of scaffold material to chondrocyte aggregate behavior. *The 24th Bioengineering Conference, 2012 Annual Meeting of BE/JSME*. (2012), Osaka

Akihisa Otaka, Yasushi Tamada, Yoshihiko Kuwana, Naoya Hatano and Naohide Tomita. Quantification of chondrocyte aggregate behavior on scaffold materials, *The 11th Congress of the Japanese Society for Regenerative Medicine*. (2012), Kanagawa.

Kazuya Takahashi, Akihisa Otaka, Yusuke Kambe, Katsura Kojima, Yasushi Tamada and Naohide Tomita. The effect of intercellular adhesion on cartilage tissue formation on fibroin substrates, *The 11th Congress of the Japanese Society for Regenerative Medicine*. (2012), Kanagawa.

Kenji Isshiki, Akihisa Otaka, Kazuya Takahashi, Yuji S Takeda, Katsura Kojima, Yasushi Tamada and Naohide Tomita. Quantitative method for evaluating the effect of cell density on cell migration, *The 11th Congress of the Japanese Society for Regenerative Medicine*. (2012), Kanagawa.

Kenji Isshiki, Akihisa Otaka, Kazuya Takahashi, Yuji S Takeda, Katsura Kojima, Yasushi Tamada and Naohide Tomita. The effect of cell density for cell aggregation behavior, *The Mechanical Engineering Congress, 2012 Japan*. (2012), Ishikawa.

Kazuya Takahashi, Akihisa Otaka, Yusuke Kambe, Katsura Kojima, Yasushi Tamada and Naohide Tomita. The effect of cell-cell adhesion for cell aggregation behavior, *The Mechanical Engineering Congress, 2012 Japan*. (2012), Ishikawa.

Kazuya Takahashi, Akihisa Otaka, Yusuke Kambe, Katsura Kojima, Yasushi Tamada and Naohide Tomita. The effect of culture environment for cell aggregation behavior, *The 23rd JSME Conference on Frontiers in Bioengineering*. (2012), Aomori.

Kenji Isshiki, Akihisa Otaka, Kazuya Takahashi, Yuji S Takeda, Katsura Kojima, Yasushi Tamada and Naohide Tomita. The relationship between cell migration directions and cell density gradients within chondrocyte aggregate formation, *The 23rd JSME Conference on Frontiers in Bioengineering*. (2012), Aomori.

Kenji Isshiki, Akihisa Otaka, Kazuya Takahashi, Yuji S Takeda, Katsura Kojima, Yasushi Tamada and Naohide Tomita. Quantitative method for evaluating the effect of cell distribution on cell migration, *The 39th Annual Meeting of the Japanese Society for Clinical Biomechanics*. (2012), Chiba.

Kazuya Takahashi, Akihisa Otaka, Yusuke Kambe, Katsura Kojima, Yasushi Tamada and Naohide Tomita. Application of quantitative method to evaluate chondrocyte aggregate formation, *The 5th Japanese Society for Quantitative Biology*. (2012), Tokyo.

Akihisa Otaka, Kenji Isshiki, Kazuya Takahashi, Katsura Kojima, Yasushi Tamada and Naohide Tomita. Quantitative method for evaluating chondrocyte aggregate formation on scaffold materials, *The 5th Japanese Society for Quantitative Biology*. (2012), Tokyo.

Akihisa Otaka, Kumpei Sano, Kenji Isshiki, Kazuya Takahashi, Katsura Kojima, Yasushi Tamada and Naohide Tomita. Verification of quantitative method for evaluating density dependent migration of cells, *The 24th JSME Conference on Frontiers in Bioengineering*. (2013), Tokyo.

Kumpei Sano, Akihisa Otaka, Kenji Isshiki, Kazuya Takahashi, Katsura Kojima, Yasushi Tamada and Naohide Tomita. The relationship between chondrocyte migration directions and positions of adjacent cells on different substrates, *The 6th Japanese Society for Quantitative Biology*. (2013), Osaka.

Akihisa Otaka and Naohide Tomita. Quantification of cell aggregate formation on fibroin substrates using co-migration analysis, *The 6th Japanese Society for Quantitative Biology*. (2013), Osaka.

Akihisa Otaka, Kenji Isshiki, Kumpei Sano, Katsura Kojima, Yasushi Tamada and Naohide Tomita. Quantitative analysis of trajectory data during cell aggregate formation, *The 26th Bioengineering Conference, 2014 Annual Meeting of BE/JSME*. (2014), Miyagi.

Supplemental data

CODE 1: CELL POSITION ANALYSIS USING VORONOI DIAGRAM

```
### Usage ###
#    a<-data.frame(x=runif(50,0,50),y=runif(50,0,50))
#    area.disorder(a)
#    area.disorder(a,plot.this=T)
#    a<-data.frame(x=c(rnorm(10,20),rnorm(10,30),runif(30,0,50)),
     y=c(rnorm(10,35),rnorm(10,20),runif(30,0,50)))
#    area.disorder(a)

if(!any(installed.packages()[,"Package"]=="tripack"))
     stop("Please install tripack package beforehand.")
require("tripack")

area.disorder <- function(x, y=NULL, plot.this=FALSE, ...){
     if (is.null(x))
          stop("argument x missing.")
     if (is.null(y)) {
          x1 <- x$x
          y1 <- x$y
          if (is.null(x1) || is.null(y1))
               stop("argument y missing and x contains no $x or $y
     component.")
     } else {
          x1 <- x
          y1 <- y
     }

     ok <- complete.cases(x1,y1)
     if(any(!ok)){
          x1 <- x1[ok]
          y1 <- y1[ok]
     }
     x1 <- x1 + rnorm(length(x1), sd=0.001)
     y1 <- y1 + rnorm(length(y1), sd=0.001)

     vcell <- voronoi.mosaic(x1,y1)
     on.cvx <- on.convex.hull(tri.mesh(x1,y1,duplicate="remove"),x1,y1)
     circ <- tri.mesh(x1[on.cvx],y1[on.cvx],duplicate="remove")
     inside <- sapply(voronoi.polygons(vcell), function(v)
     all(in.convex.hull(circ,v[,1],v[,2])))
```

```
        area <- voronoi.area(vcell)
        area <- area[-which(is.na(area))]
        area <- area[inside]

        if(plot.this){
            plot(x1,y1,type="n",asp=1, ...)
            sapply(voronoi.polygons(vcell)[inside], polygon,col='skyblue')
            plot.voronoi(vcell,do.points=F,add=T)
            convex.hull(circ, plot.it=T,add=T,col="red")
            points(x1,y1,pch=20,col="blue")
        }

        cat("mosaic area:",area,"\n")
        1-(1+sd(area)/mean(area))^(-1)
    }
```

CODE 2: ANALYSIS OF CELL CO-MIGRATION

```
mult_dist <- function(data){
    len<-nrow(data)
    from<-do.call("c",mapply(rep,1:(len-1),(len-1):1))
    to<-do.call("c",mapply(seq,2:len,len,1))
    d<-c(dist(data))
    data.frame(from,to,d)
}

# ある2細胞の近接持続時間を算出
#（入力）dist_set: 距離の連続データ, dist_thresh: 着目する距離のしきい値
#（出力）time: 継続時間, from: イベント開始フレーム, to: イベント最終フレーム
#    endpoint: 真のエンドポイント（打切りの有無), startup: 開始見過ごしの有無
duration <- function(dist_set, dist_thresh){
    dset <- c(NA,dist_set,NA) #前後に空のデータを追加
    len <- length(dset)

    # しきい値判定（しきい値以下 or 空データの場合FALSE）
    bin <- dset<dist_thresh
    bin[is.na(bin)] <- F

    # しきい値判定結果が変化するタイムポイントを算出
    from <- which( bin[-1] & !bin[-len])+1
    to   <- which(!bin[-1] &  bin[-len])+1
    startup   <- !is.na(dset[from-1])
    endpoint <- !is.na(dset[to])

    from <- from-1; # 最初の空データ分ずらす
    to   <- to-2 # 最初・最後の空データ分ずらす
```

```
        data.frame(time=to-from+1,from,to,endpoint,startup)
    }

    # 全細胞近接の持続時間を算出
    #（入力）traj: 軌跡データセット, dist_thresh: 着目する距離のしきい値
    #（出力）i,j: 細胞番号, time: 継続時間,
    #          from: イベント開始フレーム, to: イベント最終フレーム
    #    endpoint: 真のエンドポイント（打切りの有無), startup: 開始見過ごしの有無
    get.durations <- function(dist_thresh, traj){
        frm <- max(traj$frame)
        len <- max(traj$cell)-1
        i <- do.call("c",mapply(rep,1:len,len:1))
        j <- do.call("c",mapply(seq,1:len,len,1))+1
        cal.dist <- function(f){
            traj <- traj[traj$frame==f,]
            traj <- traj[sort.list(traj$cell, method="radix"),]
            dist(traj[,c("x","y")])}
        dst <- sapply(1:frm, cal.dist)
        c <- sapply(dur<-apply(dst, 1, duration, dist_thresh), nrow)
        i <- do.call("c",mapply(rep, i, c))
        j <- do.call("c",mapply(rep, j, c))
        cbind(i, j, do.call("rbind",dur))
    }


    # 距離間マトリックスの可視化関数（get.durationとは）
    visualize.dist <- function(traj, na.rm=F, time.delay=0.2){
        if(na.rm) traj <- traj[!is.na(traj$x),]
        traj <- traj[sort.list(traj$cell, method="radix"),]
        # as.matrixが便利 NAもOK
        for(i in 1:145){
            a <- traj[traj$frame==i,c("x","y")]

            image(1:length(a$x),1:length(a$x),as.matrix(dist(a)),
                col=topo.colors(255),xlab="i",ylab="j",asp=1)
            Sys.sleep(time.delay)}
    }
```

CODE 3: ANALYSIS OF CELL MIGRATION DIRECTION

```
SIZE_X    = 680                 # Image width
SIZE_Y    = 512                 # Image height

# Usage: ans<-analysis(1, 40, "folder name", "output file name")
analysis <- function(frame_span, band_width, file_dir,
    save_dir=sprintf("Result_%s", tail(strsplit(file_dir,"/")[[1]],n=1))) {
```

```
7           if(!is.numeric(frame_span) | !is.numeric(band_width)
8           | !is.character(file_dir))
9               stop("usage: analysis(frame span, band width, input directory name,
10          (output directory name) )")
11
12          # 解析
13          tdata <- import(file_dir) # 軌跡読込み
14          results <- analysis.basic(tdata, frame_span, band_width)
15
16          # 出力
17          dir.create(save_dir) # 出力用ディレクトリの作成
18          write.csv(
19              list(directory=file_dir, frame_size=max(tdata$frame),
20          frame_span=frame_span, band_width=band_width),
21              sprintf("%s/param.csv",save_dir)) # 解析条件の出力
22          sapply(1:max(tdata$frame),
23              function(n)
24          write.csv(results[results$frame==n,-1],sprintf("%s/%d.csv",save_dir,n),
25              row.names=F,na="")) # 解析結果の出力
26
27          results
28      }
29
30
31      analysis.basic <- function(traj, frame_span, band_width){
32          ncell   <- max(traj$cell)
33          nframe <- max(traj$frame)
34
35          # 移動/密度こう配 解析
36          from <- 1:(nframe-frame_span)
37          to     <- from + frame_span
38          ddm.custom <- function(w,f,t) ddm(traj, w, f, t)
39          results <- mapply(ddm.custom, band_width, from, to, SIMPLIFY=F)
40          results <- do.call("rbind",results)
41
42          # 解析範囲外の frame_span分 の空データを追加し，元の traj 列に追記
43          brank <- as.data.frame(matrix(NA,
44          nrow=frame_span*ncell,ncol=dim(results)[2]))
45          colnames(brank) <- colnames(results)
46          results <- rbind(results, brank)
47          results <- cbind(traj, results)
48
49          #近傍細胞との細胞間距離の算出
50          nearest <- lapply(1:nframe, function(i)
51          dist2(traj[traj$frame==i,c("x","y")]))
52          nearest <- do.call("c",nearest)
```

```
        results <- cbind(results, nearest)

        #トリム判定
        trimed <- trim(traj)
        results <- cbind(results, trimed)
    }


    # import関数で読み込んだ軌跡データから、from~toの細胞移動と密度勾配とのなす
        角を求める関数
    # ddm = density dependen migration
    ddm <- function(traj, bw, from, to) {

        #データの読み込み
        data1 <- traj[traj$frame==from,];
        data2 <- traj[traj$frame==to,];

        vdisp <- data2 - data1 #細胞移動の計算
        vgrad <- ddm.DensityGradCalulation(bw,data1$x,data1$y) #密度勾配の計
        算
        inner <- vdisp$x*vgrad$x + vdisp$y*vgrad$y #細胞移動と密度勾配の内積

        sdisp <- abs2D(vdisp) #細胞の移動変位
        sgrad <- abs2D(vgrad) #密度勾配の大きさ
        cos   <- inner/(sdisp*sgrad) #細胞移動と密度勾配のなす角の余弦
        theta <- acos(cos)*180/pi #細胞移動と密度勾配のなす角（度数法）

        data.frame(theta=theta,cos=cos,displacement=sdisp,gradient=sgrad)
    }


    #あるstepにおける全細胞位置での密度勾配の計算
    ddm.DensityGradCalulation <- function(band_width, x, y) {

        nx <- numeric( length(x) )
        ny <- numeric( length(x) )

        for ( mark in 1:length(x) ) {

            if(is.na(x[mark]) == TRUE) {
                nx[mark] <- NA
                ny[mark] <- NA
            } else {
                n_grad <- ddm.DensityGrad(band_width, mark, x,y)
                n_x <- (n_grad)[1]
                n_y <- (n_grad)[2]
```

```
                        nx[mark] <- n_x
                        ny[mark] <- n_y
                    }

            }

            return(list(x=nx, y=ny))
        }
```

CODE 4: R CODE FOR CELL TRAJECTORY IMPORT

```
import <- function(dir_name){
    fn <- list.files(path= dir_name, pattern="*.csv", full.names=T)
    len <- length(read.csv(fn[1])[[1]])
    traj <- lapply(fn, function(fname){ cbind(cell=1:len, read.csv(fname) ) })
    traj <- do.call("rbind", traj)
    traj <- traj[sort.list(traj$frame, method="radix"),]
    if( any(unique(traj$frame) != 1:max(traj$frame)) )
        stop("import error: missing frames")
    if( any(traj$cell != rep(1:len,max(traj$frame))) )
        stop("import error: bad alignment (need debugging!!)")
    traj
}
```

Acknowledgements

I would like to thank many people for their contribution to this study. First, I would like to express my deep gratitude to Professor Naohide Tomita my supervisors, for his patient guidance, enthusiastic encouragement and profound advisements. I could not continue this challenging project without his enormous supports.

I would like to offer my special thanks to Professor Ari Ide-Ektessabi and Professor Taiji Adachi from the Graduate School of Engineering Kyoto University who reviewed this thesis and gave me strict and enlightening advises.

I would like to express my great appreciation to Dr. Yasushi Tamada from National Institutes of Agrobiological Sciences, for preparing fibroin substrates that were used in this study. The discussions with him were crucial for this study's progress. I wish to acknowledge the help provided by Dr. Yoshihiko Kuwana and Katsura Kojima from National Institutes of Agrobiological Sciences for preparing fibroin coated plates.

Animated discussions with various people improved my study a lot. I thank Dr. Ziya Kalay and Dr. Takahiro Fujiwara from iCeMS Kyoto University, Dr. Hiroaki Nakanishi from Kyoto University, Dr. Hiroaki Takagi from Nara Medical University and Dr. Takashi Sozu from Kyoto University for enlightening discussions and advisements.

I would like to express gratitude to all my colleagues. Mr. Yuji S Takeda, Mr. Kazuya Takahashi, Mr. Kenji Isshiki, Mr, Kumpei Sano, and Mr. Yotaro Nakane helped our project very much, and I always appreciated their unstinting helps. Dr. Koji Yamamoto, Dr. Naoyoshi D Kachi, Dr. Masahiro Kawakami, Dr. Eiichi Hirakata and Dr. Yusuke Kambe, are great mentors. Mr. Alex Turner not only helped me to improve my poor English but also uplifted me with words of encouragement.

The authors thank the Institute for Frontier Medical Sciences of Kyoto University for use of their facilities. This work was supported by the Grant-in-Aid for Creative Scientific Research from the Japan Science and Technology Agency and the Agri-Health Translational Project from the Ministry of Agriculture, Forestry, and Fisheries, Japan.

Finally, I would give a special thanks to all my family.

March 2014

Akihisa Otaka

DOCTORAL THESIS

Quantitative Analyses of Cell Aggregation Behavior Using Cell Trajectory Data

Department of Mechanical Engineering and Science
Graduate School of Engineering
Kyoto University

March 2014

Akihisa Otaka